Neurobiology of Disease

A *Drosophila* Model of Neuronopathic Gaucher Disease Demonstrates Lysosomal-Autophagic Defects and Altered mTOR Signalling and Is Functionally Rescued by Rapamycin

Kerri J. Kinghorn,[1,2] Sebastian Grönke,[3] Jorge Iván Castillo-Quan,[1,2,3] Nathaniel S. Woodling,[1] Li Li,[1,2] Ernestas Sirka,[4] Matthew Gegg,[5] Kevin Mills,[4] John Hardy,[2] Ivana Bjedov,[6] and Linda Partridge[1,3]

[1]Institute of Healthy Ageing and Department of Genetics, Evolution and Environment, University College London, London WC1E 6BT, United Kingdom, [2]Institute of Neurology, University College London, London WC1N 3BG, United Kingdom, [3]Max Planck Institute for Biology of Ageing, D-50931 Köln, Germany, [4]Centre for Translational Omics, Institute of Child Health, University College London, London WC1N 1EH, United Kingdom, [5]Clinical Neuroscience, Institute of Neurology, University College London, London NW3 2PF, United Kingdom, and [6]University College London Cancer Institute, London WC1E 6DD, United Kingdom

Glucocerebrosidase (*GBA1*) mutations are associated with Gaucher disease (GD), an autosomal recessive disorder caused by functional deficiency of glucocerebrosidase (GBA), a lysosomal enzyme that hydrolyzes glucosylceramide to ceramide and glucose. Neuronopathic forms of GD can be associated with rapid neurological decline (Type II) or manifest as a chronic form (Type III) with a wide spectrum of neurological signs. Furthermore, there is now a well-established link between *GBA1* mutations and Parkinson's disease (PD), with heterozygote mutations in *GBA1* considered the commonest genetic defect in PD. Here we describe a novel *Drosophila* model of GD that lacks the two fly *GBA1* orthologs. This knock-out model recapitulates the main features of GD at the cellular level with severe lysosomal defects and accumulation of glucosylceramide in the fly brain. We also demonstrate a block in autophagy flux in association with reduced lifespan, age-dependent locomotor deficits and accumulation of autophagy substrates in dGBA-deficient fly brains. Furthermore, mechanistic target of rapamycin (mTOR) signaling is downregulated in dGBA knock-out flies, with a concomitant upregulation of *Mitf* gene expression, the fly ortholog of mammalian *TFEB*, likely as a compensatory response to the autophagy block. Moreover, the mTOR inhibitor rapamycin is able to partially ameliorate the lifespan, locomotor, and oxidative stress phenotypes. Together, our results demonstrate that this *dGBA1*-deficient fly model is a useful platform for the further study of the role of lysosomal-autophagic impairment and the potential therapeutic benefits of rapamycin in neuronopathic GD. These results also have important implications for the role of autophagy and mTOR signaling in GBA1-associated *PD*.

Key words: autophagy; *Drosophila*; Gaucher disease; glucocerebrosidase; mTOR; rapamycin

Significance Statement

We developed a *Drosophila* model of neuronopathic GD by knocking-out the fly orthologs of the *GBA1* gene, demonstrating abnormal lysosomal pathology in the fly brain. Functioning lysosomes are required for autophagosome-lysosomal fusion in the autophagy pathway. We show *in vivo* that autophagy is impaired in dGBA-deficient fly brains. In response, mechanistic target of rapamycin (mTOR) activity is downregulated in dGBA-deficient flies and rapamycin ameliorates the lifespan, locomotor, and oxidative stress phenotypes. *dGBA* knock-out flies also display an upregulation of the *Drosophila* ortholog of mammalian *TFEB*, *Mitf,* a response that is unable to overcome the autophagy block. Together, our results suggest that rapamycin may have potential benefits in the treatment of GD, as well as PD linked to *GBA1* mutations.

Introduction

Homozygous mutations in the glucocerebrosidase gene (*GBA1*) can cause Gaucher disease (GD), the commonest lysosomal storage disorder. *GBA1* encodes glucocerebrosidase (GBA, also known as glucosylceramidase [GCase]), which mediates the lysosomal hydrolysis of glucosylceramide to form ceramide and glucose. Loss of GBA activity leads to lysosomal accumulation of glucosylceramide and its nonacylated analog glucosylsphingosine in a number of cell types,

Received Dec. 18, 2015; revised Aug. 17, 2016; accepted Sept. 6, 2016.

Author contributions: K.J.K., S.G., J.I.C.-Q., N.S.W., J.H., I.B., and L.P. designed research; K.J.K., S.G., J.I.C.-Q., N.S.W., E.S., L.L., M.G., and K.M. performed research; K.J.K., S.G., J.I.C.-Q., N.S.W., L.L., E.S., and M.G. analyzed data; K.J.K., J.H., and L.P. wrote the paper.

K.J.K., L.P., and J.H. were supported by the Wellcome Trust. This work was supported by Wellcome Trust MRC strategic neurodegenerative disease initiative award WT089698. K.J.K. received a postdoctoral Wellcome Trust fellowship 090541/Z/09/Z. L.P., S.G., L.L., and J.I.C.-Q. were supported by the Max Planck Society. L.L. received a Parkinson's UK PhD studentship H-1105. J.I.C.-Q. was supported by UCL Scholarships. I.B. was supported by an ERC

including macrophages and neurons, giving rise to the visceral and neurological manifestations of GD, respectively (Cox, 2010). GD is classified into three clinical subtypes based on the absence (Type I) or presence (Types II and III) of neurological involvement. Type II, or acute neuronopathic GD, is rare but results in rapidly progressive neurological decline, with a wide spectrum of clinical signs and death in infancy or early childhood. Type III, or chronic neuronopathic GD, is a more slowly progressive disorder with neurological features, including eye movement abnormalities, myoclonic epilepsy, ataxia, and dementia (Sidransky, 2004). There are currently no therapies available that target the neuronal pathology associated with GD because existing treatments, such as recombinant enzyme replacement therapy, fail to permeate the blood–brain barrier (Cox, 2010).

As well as causing GD, heterozygous *GBA1* mutations are now well-established genetic risk factors for PD and other synucleinopathies, characterized by the presence of intraneuronal aggregates called Lewy bodies (LBs), predominantly containing α-synuclein as well as ubiquitin (Shults, 2006). Both loss-of-function and gain-of-function hypotheses have been put forward to explain how mutations in *GBA1* lead to lysosomal dysfunction and neurodegeneration, and there is mounting evidence in support of the loss of GBA function hypothesis (Kinghorn, 2011). Lysosomal dysfunction in GD has far-reaching implications, not only for the degradation of α-synuclein, but also for the autophagic degradation of other superfluous or damaged cellular material and organelles, as the fusion of lysosomes with autophagosomes is a critical step in the autophagic pathway (Ravikumar et al., 2010). The process of macroautophagy can be divided into key stages, including initiation, elongation, and maturation of autophagosomes, followed by the fusion with lysosomes.

In keeping with the importance of lysosomes in the autophagy pathway, it was recently shown in macrophages and induced pluripotent stem cell (iPSC)-derived neuronal cells from GD patients that autophagy is impaired (Awad et al., 2015; Aflaki et al., 2016). Furthermore, this defect in autophagy was shown to trigger inflammasome activation and the production of inflammatory cytokines (Aflaki et al., 2016). Moreover, Osellame et al. (2013) demonstrated that there is accumulation of dysfunctional and fragmented mitochondria in a neuronopathic mouse model of GD, thought to be secondary to autophagic and proteasomal defects.

To further understand the mechanisms linking loss of GBA activity to neurodegeneration in neuronopathic GD, and also to determine whether autophagy plays a role in neurons *in vivo*, we developed a novel *Drosophila* model that lacks the two *GBA1* orthologs, *dGBA1a* and *dGBA1b*. The fruit fly has proven to be a useful model system for studying neurodegenerative diseases (Kinghorn et al., 2015) and lysosomal storage disorders, including those affecting the nervous system, such as neuronal ceroid lipofuscionoses (Myllykangas et al., 2005; Hindle et al., 2011). It is therefore a useful model for studying the mechanisms of pathogenesis of GD as well as the role of *GBA1* in neurodegeneration.

The dGBA knock-out flies proved to be faithful models of GD, with significant lysosomal dysfunction and buildup of the dGBA substrate, glucosylceramide, in the fly brain. Furthermore, there was significant neuronal autophagy impairment, which was associated with reduced survival and age-dependent locomotor abnormalities. At the cellular level, we demonstrated accumulation of p62 and polyubiquitinated proteins, both of which accumulate to form LBs in PD (Zatloukal et al., 2002), in addition to mitochondrial abnormalities. Moreover, dGBA-deficient flies displayed decreased mechanistic target of rapamycin (mTOR) signaling with a reduction in p70 S6 kinase (S6K) phosphorylation, and the mTOR inhibitor rapamycin was able to partially ameliorate the neurodegenerative phenotypes. Our results thus show an important role of autophagy and mTOR signaling in GD, and provide a useful model for the further study of pathogenic mechanisms downstream of lysosomal dysfunction.

Materials and Methods

Fly stocks and husbandry. All fly strains used were backcrossed at least 6 generations into the w^{1118} background to obtain isogenic lines. All fly stocks were maintained at 25°C on a 12:12 h light: dark cycle at constant humidity on a standard sugar-yeast medium (15 g/L-1 agar, 50 g/L-1 sugar, 100 gl-1 autolyzed yeast, 3g/L nipagin, and 3 ml/L propionic acid). For all experiments, flies were raised at a controlled density on standard sugar-yeast medium in 200 ml bottles.

Generation of dGBA1a *and* dGBA1b *mutants by ends-out homologous recombination.* The genes encoding *dGBA1a* (CG31148) and *dGBA1b* (CG31414) are located in close proximity on *Drosophila* chromosome 3, separated by the *CG31413* gene (see Fig. 1*A*). We generated specific mutants for *dGBA1a, dGBA1b* and a *dGBA1a* and *dGBA1b* double-mutant, without affecting the coding sequence of CG31413 by ends-out homologous recombination (Gong and Golic, 2004). *dGBA1a* was mutated by replacing the whole ORF with a $white^{hs}$ marker gene. *dGBA1b* was mutated by introducing a stop codon and a subsequent frame shift mutation 12 bp downstream of the predicted ATG start codon. In addition, an EcoRV restriction site was introduced to allow PCR screening of the introduced mutations. To clone the donor construct for homologous recombination, ~4 kb of 5′ and 3′ flanking sequences of the *dGBA1a* gene were cloned into the pBluescript II SK+ vector (Stratagene) by ET recombination using BAC clone CH321–50J5 (BACPAC Resource Center, Oakland, California) as template and primers SOL474/475 and SOL476/477 for the 5′ and 3′ arms, respectively. Mutations in the 3′ arm were introduced using the QuikChange site-directed mutagenesis kit (Agilent Technologies) and primers SOL482/483. Both 5′ and 3′ homologous arms were subcloned into the pW25 vector (Gong and Golic, 2004) and full-length sequenced. pW25 was obtained from the *Drosophila* Genomics Resource Centre. The dGBA donor construct was transformed into the germline of *Drosophila melanogaster* by P-element-mediated germ line transformation using the Best Gene *Drosophila* Embryo Injection Service. Crosses for ends-out homologous recombination were performed according to the rapid targeting scheme (Gong and Golic, 2004). Subsequently, the $white^{hs}$ marker gene was genetically mapped and homologous recombination events were identified by PCR. Point mutations introduced into *dGBA1b* were identified by PCR with primers SOL484 and SOL485 and subsequent digestion with EcoRV, which results in two specific DNA fragments of 120 and 193 bp from the uncut 313 bp wild-type DNA fragment. Oligonucleotide primers used for cloning and genotyping are listed in Table 1.

qRT-PCR. Total RNA was extracted from 25 heads or 25 thoraces and abdomens of 6-d-old adult flies per sample using Trizol (Invitrogen) and further purified over an RNeasy Mini column (QIAGEN) with on-column DNase digestion. cDNA was prepared from 2.5 μg RNA using the SuperScript Vil cDNA synthesis kit (Invitrogen). qRT-PCR data were performed with TaqMan primers (Applied Biosystems) in a 7900HT

Starting Grant 311331. We thank all members of the L.P. laboratory for helpful discussions and advice (especially Drs Fiona Kerr and Teresa Nicoli); Dr. Manolis Fanto (Kings College London) for help with interpretation of the electron micrographs; and Dr Kerrie Venner (Institute of Neurology Electron Microscopy Unit) for technical help with electron microscopy. We also thank Dr. Alex Whitworth, University of Cambridge, for useful discussions.

The authors declare no competing financial interests.

This article is freely available online through the *J Neurosci* Author Open Choice option.

Correspondence should be addressed to either Dr. Kerri J. Kinghorn or Professor Dame Linda Partridge, Institute of Healthy Ageing and Department of Genetics, Environment and Evolution, University College London, London WC1E 6BT, United Kingdom. E-mail: k.kinghorn@ucl.ac.uk and l.partridge@ucl.ac.uk.

DOI:10.1523/JNEUROSCI.4527-15.2016

Table 1. The oligonucleotide primers used for cloning and genotyping in the generation of the dGBA knockout flies

Name	Gene	Sequence	RS	Comment
SOL474	*GBA1a*	TTCGTAAACAATTTATTTTTCCGATAAAATTCGAATCTCCTATTATTAAACGTACGcacaacatacgagccggaagcata	BsiWI	ET Rec
SOL475	*GBA1a*	CTCCAGTTGCGTTTTGCCAAAAGAACCAGGTGTCAATCAGGTGGCAGCGTGGCGCGCCatgtgcgcggaacccctatttg	AscI	ET Rec
SOL476	*GBA1a*	AACATGTCTTTATTTAATTTTTTGTTTTGTTTAGAAAAAATAAGTTTTCAGCATGCcacaacatacgagccggaagcata	SphI	ET Rec
SOL477	*GBA1a*	CGCTCCTCCCGCAACAATTCGCTGAACTACTTGGATGGCCTAGCTGTTCAGCGGCCGCatgtgcgcggaacccctatttg	NotI	ET Rec
SOL482	*GBA1b*	ATGCCAGATATCTAGTACACCACTGCTTGG		
SOL483	*GBA1b*	CCAAGCAGTGGTGTACTAGATATCTGGCAT		
SOL484	*GBA1b*	ATTCGCCGGTCCGGCTGCTT		
SOL485	*GBA1b*	CTGCAATGCGTTTCATTTGAGG		
SOL804	*CG31468*	TAATCTACGCCCAGCCCACTTG		
SOL846	*CG31468*	ACGCTGCCACCTGATTGACA		
SOL847	*GBA1a*	ATGGGAAAAATGTTCGCCAGC		
SOL848	*GBA1a*	CTGTACAGCAGAGTGTGAATGG		
SOL850	*CG31413*	CATCAGTGGCAGTTTACCAGTC		
SOL851	*CG31413*	AAGCAGCCGGACCGGCGAAT		

real-time PCR system (Applied Biosystems). The TaqMan primers used were as follows: Dm02150554_m1 for *dGBA1b*, Dm02143806_g1 for *dGBA1a*, Dm02150538_s1 for CG31413, and a custom-made probe against Rpl32. For each sample, 4 biological replicates and 4 technical replicates were used. Relative expression was calculated using the ΔΔCT method and Rpl32 as normalization control.

For assessment of *Mitf* and *Atg8a* gene expression levels, total RNA was extracted from 20–25 fly heads per sample using TRIzol (Invitrogen) according to the manufacturer's instructions. Then 5 μg of total RNA was subjected to DNA digestion using DNase I (Ambion), immediately followed by reverse transcription using the SuperScript II system (Invitrogen) with oligo(dT) primers. qPCR was performed using the PRISM 7000 sequence-detection system (Applied Biosystems) and SYBR Green (Invitrogen) by following the manufacturer's instructions. Each sample was analyzed in duplicate, and values are the mean of the 3 or 4 independent biological repeats. The primers used were as follows: *atg8*, ATTCC ACCAACATCGGCTAC and GCCATGCCGTAAACATTCTC; *Mitf*, GC GTTCTTCTTCAGGGATTG and ACTTACGCTCGGCGAAATAG; and RP49, ATCGGTTACGGATCGAACAA and GACAATCTCCTTGCG CTTCT.

Lifespan, climbing, and fecundity analyses. The survival, climbing, and fecundity assays were performed as previously described (Kinghorn et al., 2015). For the lifespan experiments, 150 female flies (unless otherwise stated) were housed in groups of 15 and the flies were transferred every 2–3 d onto fresh food and the number of dead flies recorded.

Feeding assay (proboscis extension). Feeding rates of flies were measured using a proboscis-extension assay in undisturbed conditions as previously described (Wong et al., 2009). Briefly, flies were housed in groups of 5 per vial and kept undisturbed for 24 h before recording observation. Feeding rate was scored by a brief but continuous observation for at least 1 h of the number of flies actively extending their proboscis on the fly medium. Observation recordings were made blindly. Feeding ability was calculated by the number of feeding events divided by the number of flies in the vial over the time period measured and then by averaging this for all of the vials per genotype.

Stress experiments and rapamycin treatment. For all stress assays, flies were reared and housed as for lifespan experiments, and oxidative stress and starvation assays were performed as previously described (Kinghorn et al., 2015). Rapamycin (LC Laboratories) was dissolved in 100% ethanol to give a 50 mM stock concentration. It was then added to the standard fly medium to give the desired final concentration. Equivalent volumes of vehicle were supplemented to the medium to compensate for dilution.

Measurement of dGBA activity. dGBA activity was measured using a similar method to that previously described (Davis et al., 2016). Briefly, 20 fly heads of each genotype were homogenized and debris cleared by centrifugation. Lysates (7.5 μg protein) were mixed with 0.1 M sodium acetate, pH 4.5, and 5 mM 4-methyllumbelliferyl-β-D-glucopyranoside and incubated at 37°C. The reaction was stopped with 0.25 M glycine buffer, pH 10.4, and fluorescence measured on fluorescent plate reader (excitation, 360 nm; emission, 460 nm). dGBA activity was also measured in the presence of the inhibitor conduritol-β-epoxide (100 μM) and dGBA activity calculated as total GBA activity minus CBE-sensitive GBA activity and expressed as pmol/h/mg protein. Approximately 50% of the total dGBA activity was abolished by incubation with conduritol-β-epoxide in w^{1118} control flies.

Measurement of glucosylceramide levels. Fly heads ($n = 70$) were analyzed for glucosylceramide accumulation. The substrate was extracted in 500 μl of chloroform/methanol (2:1 v/v) containing 80 μg/ml of d4-C16:0-glucosylceramide internal standard, which was synthesized in house (Mills et al., 2005). The samples were shaken for 30 min at room temperature before the addition of 100 μl of PBS for phase separation. After a 10 min centrifugation at 16,000 × *g*, upper and lower phases were collected and 5 μl of each was injected into the ultra-performance liquid chromatography-tandem mass spectrometry system. Synthetic glucosylceramide standard (Matreya) was also analyzed to confirm analyte identity.

The samples were injected onto Waters ACQUITY UPLC system operated in partial loop mode and separated on Waters ACQUITY UPLC BEH C18 column (130Å, 1.7 μm, 2.1 mm × 50 mm) under the following gradient conditions: 0.00–0.20 → 80% A; 0.20–5.00 → 0.1% A; 5.00–9.00 → 0.1% A; 9.01–11.00 → 80% A, where mobile Phase A was ddH_2O [0.1% FA] and Phase B was methanol. Column and sample temperatures were kept at 40°C and 10°C, respectively. Weak wash solvent was ddH_2O (0.1% FA), and strong wash solvent was acetonitrile: methanol:isopropanol:ddH_2O (1:1:1:1 v/v). The eluting analytes were detected on a Waters XEVO TQ-S triple quadrupole mass spectrometer, which was equipped with the electrospray ion source and operated in MRM and positive ion mode with the tune page parameters set to achieve the maximum sensitivity for glycosphingolipids as described previously (Auray-Blais et al., 2015). The data were processed with MassLynx version 4.1.

Measurement of lysosomal enzymes. Twenty flies were homogenized in RIPA buffer (150 mM NaCl, 50 mM Tris, pH 8.0, 1% (v/v) NP-40, 1% (w/v) sodium deoxycholate, 0.1% (w/v) SDS, protease inhibitor mixture) with a micro-pestle. Debris was pelleted at 17, 000 × *g* and protein concentration of the supernatant was determined using the protein BCA kit (Pierce). β-Hexosaminidase activity (10 μg protein) was measured in McIlvaine citrate buffer, pH 4.2, with 2 mM 4-methylumbelliferyl-*N*-acetyl-glucosamide substrate. β-Galactosidase activity (10 μg protein) was measured in McIlvaine citrate buffer, pH 4.1, with 0.25 mM 4-methylumbelliferyl-β-D-galactopyransoside substrate. Both enzyme assays were incubated at 37°C for 30 min and the reaction stopped by addition of 0.25 M glycine, pH 10.4. Fluorescent product was measured using a plate reader (excitation, 340 nm; emission, 460 nm) and compared against 1 nmol 4-methyllumbelliferone standard.

Triacylglyceride and ATP assays. Levels of triacylglyceride (TAG) in adult females were measured using the Triglyceride Infinity Reagent (Thermo Scientific) and normalized to total body protein using a BCA assay (Sigma). The ATP concentration of whole female flies was determined using the ATP Bioluminescence Assay Kit HS II (Roche) as previously described (Kinghorn et al., 2015).

Antibodies and Western blotting. For Atg8 Western blotting, 10 to 15 fly heads or 5 headless bodies were homogenized in 2 × Laemmli loading buffer (100 mM Tris 6.8, 20% glycerol, 4% SDS) containing 5% β-mercaptoethanol and then boiled for 5 min. Approximately 40 μg of protein extract was loaded per lane. Proteins were separated on SDS polyacrylamide gels and transferred to a nitrocellulose membrane. For ubiquitin Western blots, 12 fly heads per sample were homogenized in Triton-X buffer (1% Triton-X, 10 mM NEM, 50 μm MG132, Complete Mini protease inhibitors, Roche, in PBS). After centrifugation, the insoluble pellet was resuspended in SDS buffer (2% SDS, 10 mM NEM, 50 μm MG132, complete mini protease inhibitors, Roche, 50 mM Tris, pH 7.4), centrifuged, and the supernatant collected as the insoluble sample for Western blot. Proteins were separated on 4%–12% NuPage Bis-Tris gels (Invitrogen) and transferred to a PVDF membrane. The membranes were then blocked in 5% BSA in TBST (TBS with 0.05% Tween 20) for 1 h at room temperature, after which they were probed with primary antibodies diluted in 5% BSA in TBST overnight at 4°C. Blots were developed using the ECL detection system. The following primary antibodies were used: β-actin (Abcam, #ab1801; 1:5000), mouse anti-polyubiquitinated proteins (clone FK2, Millipore, 1:1000) and anti-Atg8 (1:1000) (Castillo-Quan et al., 2016).

For detection of S6K and tS6K protein levels, 15 fly heads in each sample were prepared by homogenization in 2 × SDS Laemmli sample buffer (4% SDS, 20% glycerol, 120 mM Tris-HCl, pH 6.8, 200 mM DTT with bromophenol blue), and boiled at 95°C for 5 min. Samples were separated on precast 4%–12% Invitrogen Bis-Tris gels (NP0322) and blotted onto nitrocellulose paper in Tris-glycine buffer supplemented with 10% ethanol. They were then blocked as above, and the primary antibodies used were anti-phosphorylated S6K anti-phospho-Thr398-S6K (Cell Signaling Technology, #9209, 1:1000), anti-total-S6K (1:1000) (Sofola-Adesakin et al., 2014). The appropriate secondary antibodies (Abcam) were diluted 1:10,000 in 5% BSA in TBST for 1 h at room temperature. Bands were visualized with Luminata Forte (Millipore).

All blots were imaged with ImageQuant LAS4000 (GE Healthcare Life Science). Quantification was performed using the ImageJ program (National Institutes of Health).

Immunohistochemistry, LysoTracker, confocal imaging, and quantification. For immunohistochemistry, adult brains were dissected in PBS and immediately fixed in cold 4% PFA (v/v) for 20 min at room temperature. After fixation, the samples were washed in PBT (PBS containing 0.3% Triton X-100, v/v) four times for 20 min then blocked in PBT containing 10% BSA (PBT-BSA) for 2 h at 20°C-30°C. For primary antibody treatment, samples were incubated in PBT-BSA containing the primary antibody for 3 d at 4°C. After primary antibody incubation, brains were washed in PBT, four times for 20 min at 20°C-30°C, then incubated in PBT-BSA containing the secondary antibody for 24 h at 4°C. Brains were washed four times with PBT for 20 min at 20°C-30°C. Brains were finally mounted in Vectashield containing DAPI overnight (Vector Laboratories). Antibodies were used at the following dilutions: rabbit anti-Ref(2)P (Abcam) 1:200; mouse anti-polyubiquitinated proteins (FK2, Millipore) 1:200; mouse anti-Bruchpilot (DSHB antibody nc82), 1:100; secondary goat anti-rabbit AlexaFluor-568 1:250, and secondary goat-anti-mouse AlexaFluor-488 1:250.

For Ref(2)P and ubiquitin staining, image stacks of specimens were obtained on a Zeiss LSM700 confocal microscope using a 10 × objective for whole-brain imaging. Stacks of 7.25 μM *Z* distance and 14 images per stack were taken. Images were quantified using ImageJ software. Briefly, confocal stacks were merged into a single plane by using the maximum projection function. A region of each central brain was manually selected (200 μm high, 100 μm wide) from the dorsal to the ventral aspect of the brain. Thresholds were then set for p62/Ref(2)P and ubiquitin, and the area above threshold within this region was measured.

For Bruchpilot staining, image stacks were obtained using a 40 × objective in the region encompassing the ventral edge of the antennal lobe and dorsal edge of the subesophageal ganglion. Stacks of 1.00 μM *Z* distance and 11 images per stack were taken. Images were quantified using ImageJ software. Briefly, confocal stacks were merged into a single plane by using the average projection function. Two regions of each image were manually selected (10 μm high, 10 μm wide), one in the center of the antennal lobe region and one in the center of the suboesphageal ganglion region, by an observer blinded to genotype. The mean intensity of Bruchpilot staining was then measured for each region of interest.

For LysoTracker staining, adult brains were dissected in PBS and immediately transferred to a solution of PBS with 1 μM LysoTracker Red DND-99 (Invitrogen) and 1 μM DAPI. Brains were mounted on slides in this solution and imaged within 15 min of dissection on a Zeiss LSM700 confocal microscope using a 40 × objective. For each replicate within the experiment, one control and one mutant brain were imaged side by side, with identical microscope settings and images taken from the same region of the subesophageal ganglion for each brain. Images were quantified using ImageJ software, by setting a threshold for LysoTracker and measuring the area above threshold.

Electron microscopy of fly brains and image analysis. The flies were decapitated and the proboscis removed to allow penetration of the fixative. They were then processed and visualized using previously described methods (Kinghorn et al., 2015). Cross-sectional mitochondrial and rhabdomere areas were measured manually using ImageJ software.

Statistical analyses. Survival experiments were analyzed using log rank test. Single comparisons were analyzed using the Student's *t* test. Other data were tested by ANOVA, and planned comparisons of means were made using Tukey-Kramer HSD test. Statistical analyses were performed using Excel, GraphPad Prism, or JMP software version 9 (SAS Institute).

Results

Knock-out of the *Drosophila* orthologs of GBA1 using homologous recombination

Drosophila melanogaster has two orthologs of the human *GBA1* gene, CG31148 and CG31414, which we refer to as *dGBA1a* and *dGBA1b*, respectively. These two genes are found on the same chromosome, separated by the *CG31413* gene (Fig. 1*A*), and show differential tissue expression. *dGBA1b* is expressed in the adult brain, albeit at low levels, as well as moderately expressed in the adult fat body. *dGBA1a* is predominantly expressed in the adult fly digestive system and shows no expression in the adult brain (Flyatlas) (Robinson et al., 2013). To study the function of the *dGBA1* genes, we produced loss-of-function mutants lacking *dGBA1a* ($dGBA1a^{-/-}$), d*GBA1b* ($dGBA1b^{-/-}$), or double-mutants lacking both genes ($dGBA1a,b^{-/-}$) using ends-out homologous recombination. The complete open reading frame of *dGBA1a* was knocked out by homologous recombination, whereas *dGBA1b* expression was disrupted by the introduction of a stop codon and a frame shift 12b downstream of the putative ATG start codon (Fig. 1*A*; for more details, see Materials and Methods). Deletion of *dGBA1a* and integrity of the *CG31413* gene were confirmed by PCR on genomic DNA (Fig. 1*B*). Furthermore, introduction of specific point mutations within the *dGBA1b* gene were verified by PCR (Fig. 1*C*) and sequencing. To test whether these mutations affected expression of the *dGBA* genes and the interjacent *CG31413* gene, we measured mRNA transcript levels by qRT-PCR data in female heads and bodies for *dGBA1b* (Fig. 1*D*), in female bodies for *dGBA1a* (Fig. 1*E*), and in male bodies for *CG31413* (Fig. 1*F*). The latter gene is specifically expressed in male accessory glands (Flyatlas) (Robinson et al., 2013). *dGBA1b* transcript levels were barely detected in $dGBA1b^{-/-}$ single-mutant and $dGBA1a,b^{-/-}$ double-mutant flies (Fig. 1*D*), suggesting that the introduced point mutations affect the stability of the *dGBA1b* transcript. *dGBA1a* expression was absent from $dGBA1a^{-/-}$ single-mutant and $GBA1a,b^{-/-}$ double-mutant flies (Fig. 1*E*) and *CG31413* expression was slightly reduced in $dGBA1a,b^{-/-}$ double-mutants (Fig. 1*F*). Thus, the qRT-PCR data suggest that both $dGBA1a^{-/-}$ and $dGBA1b^{-/-}$ are loss-of-function alleles for the respective *dGBA* genes, with the single mutations not affecting expression of the CG31413 gene, and the double mutation very slightly reducing it. Knock-out of *dGBA1a*, *dGBA1b*, or both genes was not associated with any gross changes in body size or obvious differences in morphology (data not shown). In keeping

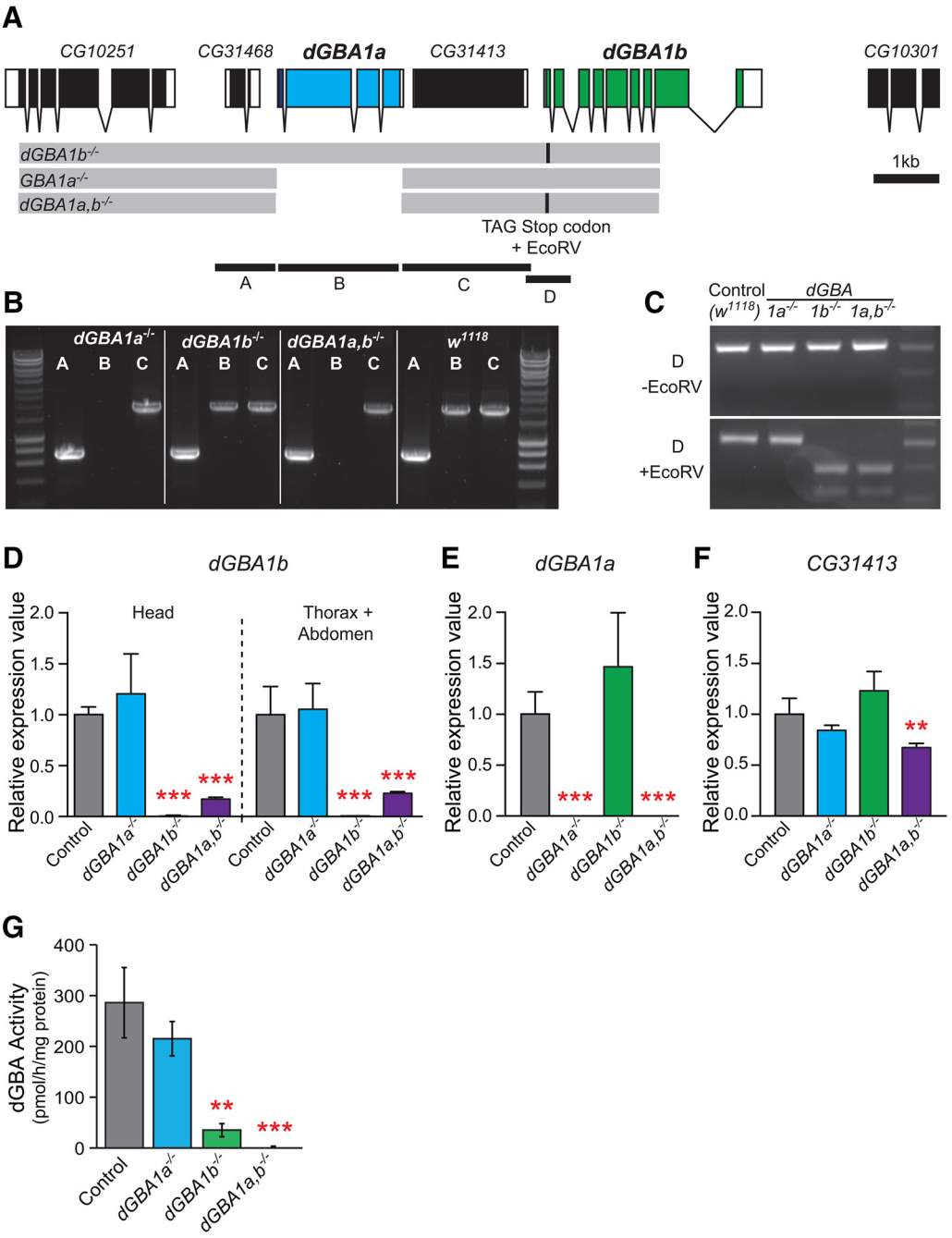

Figure 1. Generation of flies lacking the d*GBA1a* and d*GBA1b* genes. ***A***, Schematic view of the *dGBA1* gene locus. *dGBA1a* and *dGBA1b* are located in close proximity separated by the CG31413 gene, the function of which is unknown. Gray bars represent donor constructs for ends-out homologous recombination. Gaps between gray bars indicate genomic regions replaced by a *white*^{hs} marker gene. Black boxes represent coding parts of exons. White boxes represent noncoding regions. *dGBA1a* was mutated by introduction of a stop codon and a frame shift 12 kb downstream of the ATG start codon. Black bars ***A–D*** represent genomic regions PCR amplified in ***B***, ***C***. ***B***, PCR on genomic DNA of *dGBA1b*$^{-/-}$, *dGBA1a*$^{-/-}$, *dGBA1a, b*$^{-/-}$ mutants and w^{1118} control flies. ***C***, PCR verification of point mutations in *dGBA1b* mutants. An EcoRV restriction site accompanied the introduced stop codon and frame shift mutation. Top, Undigested PCR product. Bottom, PCR product restricted with EcoRV. A specific double band is apparent only in *dGBAb*$^{-/-}$ and *dGBA1a, b*$^{-/-}$ mutants. ***D–F***, Quantitative real-time PCR with probes directed against *dGBA1b* (***D***), *dGBA1a* (***E***), and CG31413 (***F***). Total RNA was isolated from female heads (left) and bodies (right) (***D***), female bodies (***E***), and male bodies (***F***). Tissue and gender were chosen corresponding to the endogenous expression of the respective gene. ***D–F***, $^{**}p \leq 0.01$ (one-way ANOVA with Dunnett's test relative to w^{1118} controls). $^{***}p \leq 0.001$ (one-way ANOVA with Dunnett's test relative to w^{1118} controls). ***G***, dGBA activity in fly heads was decreased by ~95% in *dGBA1b*$^{-/-}$ flies ($^{**}p = 0.01$) and was undetectable in *dGBA1a,b*$^{-/-}$ flies ($^{***}p = 0.006$). Conversely, the dGBA activity measured in *dGBA1a*$^{-/-}$ fly heads was not significantly different from that of controls ($p = 0.39$).

with the expression of *dGBA1b*, and not *dGBA1a*, in the fly brain, dGBA activity levels were decreased by 95% in *dGBA1b*$^{-/-}$ fly heads and were undetectable in the heads of *dGBA1a,b*$^{-/-}$ flies. Conversely, the levels of dGBA activity in *dGBA1a*$^{-/-}$ fly heads were not statistically different from that of controls, consistent with its predominant expression within the fly midgut (Fig. 1*G*).

Flies lacking dGBA displayed reduced lifespan and progressive age-dependent locomotor deficits

The lifespan of flies lacking *dGBA1a* (*dGBA1a*$^{-/-}$), *dGBA1b* (*dGBA1b*$^{-/-}$) or both *dGBA1* genes (*dGBA1a,b*$^{-/-}$) was assessed. *dGBA1b*$^{-/-}$ flies displayed reduced survival compared with control flies. However, *dGBA1a*$^{-/-}$ flies, which lack the *dGBA* isoform ex-

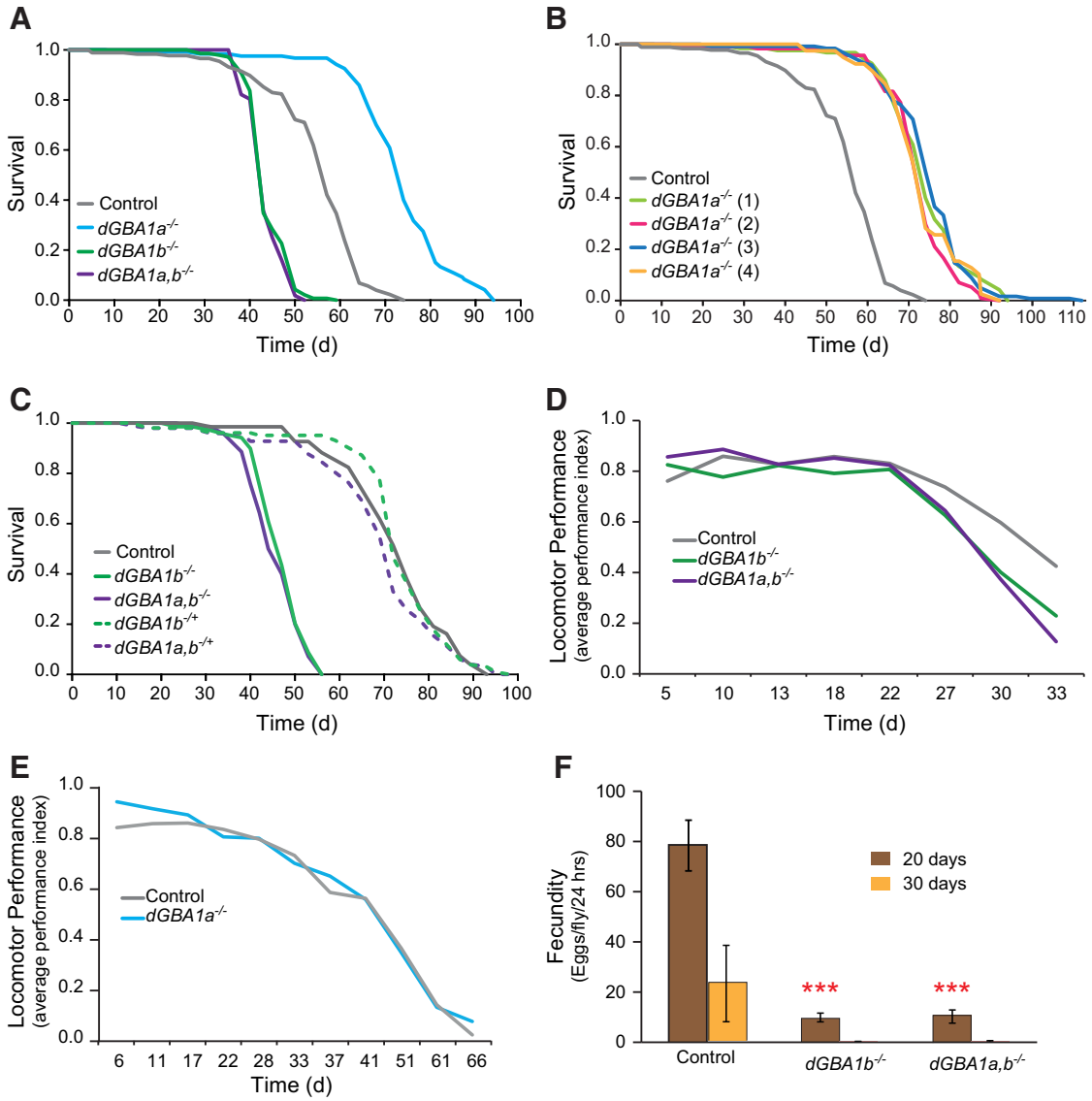

Figure 2. Lack of *dGBA* activity led to reduced survival and locomotor deficits. ***A***, *dGBA1b*$^{-/-}$ and *dGBA1a,b*$^{-/-}$ female flies had significantly reduced lifespan compared with w^{1118} control flies ($p = 3 \times 10^{-39}$ and $p = 7 \times 10^{-27}$). Furthermore, *dGBA1a*$^{-/-}$ flies displayed a significant lifespan extension compared with control flies ($p = 8 \times 10^{-52}$). ***B***, This lifespan extension was consistent using a further 4 independent *dGBA1a*$^{-/-}$ lines (all $p < 6 \times 10^{-12}$, $n = 150$ flies per genotype). ***C***, Flies heterozygous for *dGBA1b* or both *dGBA1* genes (*dGBA1b*$^{-/+}$ and *dGBA1a,b*$^{-/+}$) did not display a lifespan phenotype ($p = 0.69$ and $p = 0.33$). ***D***, *dGBA1b*$^{-/-}$ and *dGBA1a,b*$^{-/-}$ flies showed an age-dependent reduction in climbing ability compared with w^{1118} control flies ($p = 0.0001$ and $p = 0.0004$; $n = 45$ flies per genotype, 3 repeats each). ***E***, The climbing ability of *dGBA1a*$^{-/-}$ flies was indistinguishable from that of controls ($p = 0.38$). ***F***, The fecundity of *dGBA1b*$^{-/-}$ and *dGBA1a,b*$^{-/-}$ flies was significantly reduced at day 20 compared with age-matched control flies. ***$p = 3 \times 10^{-6}$. ***$p = 2 \times 10^{-5}$. They were almost completely infertile at day 30, whereas >20% of the control flies were still able to lay eggs.

pressed mainly in the digestive system, showed a significantly increased survival compared with control flies (Fig. 2*A*), and this trend was seen using 4 additional *dGBA1a* null mutant fly lines (Fig. 2*B*). Interestingly, double-mutant *dGBA1a,b*$^{-/-}$ flies displayed a lifespan that was similar to that of the single *dGBA1b* knock-out line (Fig. 2*A*), suggesting that the detrimental effects of *dGBA1b* deficiency on lifespan cannot be reversed by the prolongevity effects of *dGBA1a* knock-out. Given that *GBA1* mutations are usually found in the heterozygous state in PD and other synucleinopathies, we also assessed *dGBA1b* and *dGBA1a* heterozygote knock-out flies (*dGBA1b*$^{-/+}$ and *dGBA1a*$^{-/+}$) and found that the lifespans of these flies were not significantly different from those of controls (Fig. 2*C*).

In keeping with the lifespan phenotypes, *dGBA1b*$^{-/-}$ and *dGBA1a,b*$^{-/-}$ flies, which lack the *dGBA* isoform expressed in the brain, also displayed progressive age-dependent locomotor deficits, with the climbing ability of *dGBA1b*$^{-/-}$ and *dGBA1a,b*$^{-/-}$ flies in response to light tapping falling below that of controls at older ages (Fig. 2*D*). Knock-out of *dGBA1a*, despite its prolongevity effects, did not have any significant effect on climbing ability over time compared with control flies (Fig. 2*E*). Therefore, because loss of *dGBA1a* was not associated with any lifespan defect or change in locomotor ability, and has no expression in the adult brain, we concentrated on studying the *dGBA1b*$^{-/-}$ and *dGBA1a,b*$^{-/-}$ flies in the subsequent experiments.

We also assessed the fecundity of *dGBA1b*$^{-/-}$ and *dGBA1a,b*$^{-/-}$ female flies as a further measure of healthspan. The number of eggs laid per female significantly declined with age compared with age-matched control flies, and day 30 null mutant

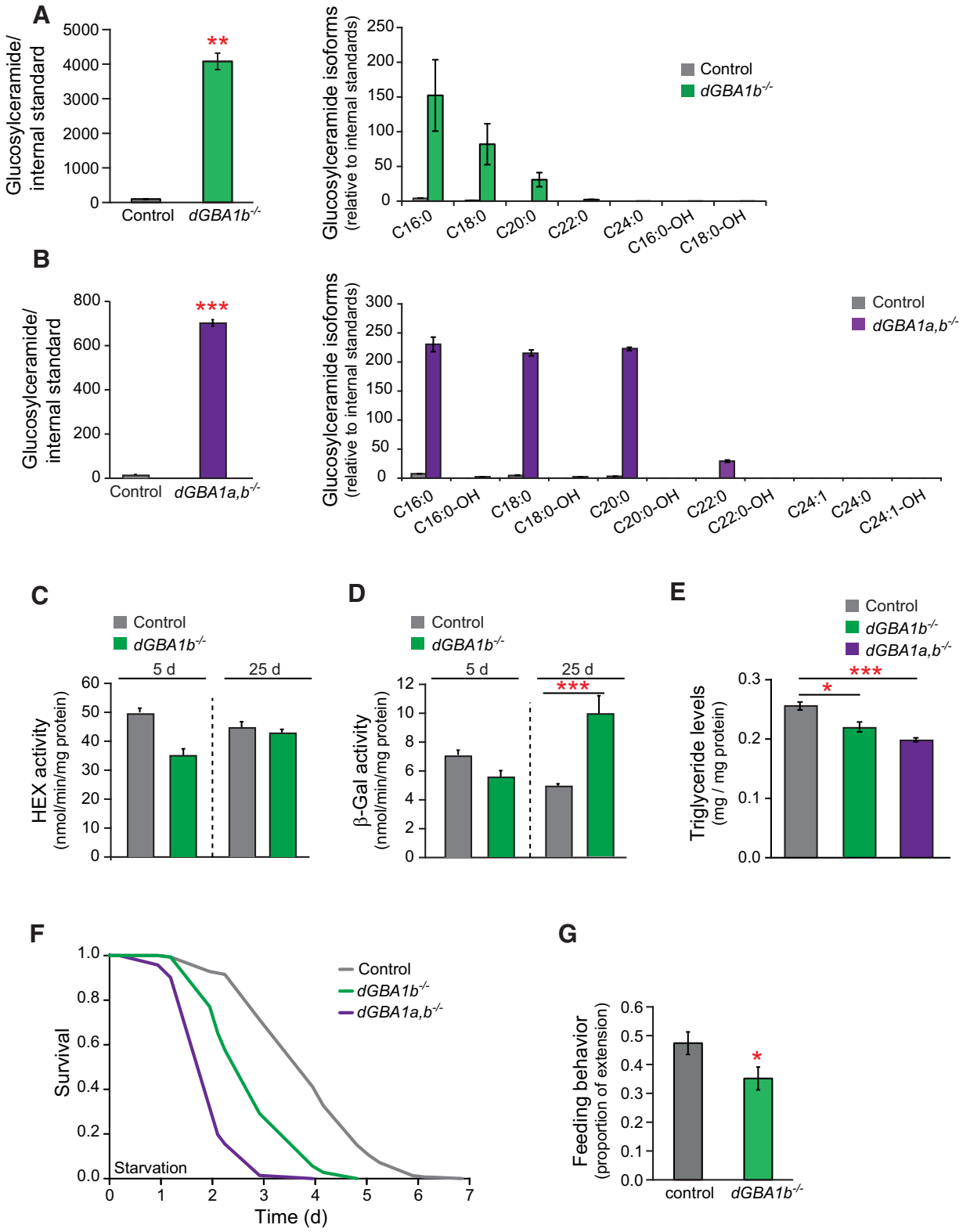

Figure 3. Loss of dGBA activity resulted in lipid defects and substrate accumulation in fly brains. ***A***, Mass spectroscopic analysis revealed an ~7-fold increase in accumulation of the dGBA substrate, glucosylceramide, in the heads ($n = 70$) of 25-d-old *dGBA1b*$^{-/-}$ compared with age-matched w^{1118} control flies. $^{**}p = 0.01$. The isoforms that were predominantly elevated were C16:0, C18:0, and C20:0. ***B***, Similar results were seen in *dGBA1a,b*$^{-/-}$ fly heads ($n = 70$ heads per sample, 3 technical repeats). $^{***}p = 0.0008$. ***C***, There was no age-dependent decrease in hexosaminidase (HEX) activity or (***D***) β-galactosidase (β-GAL) activity in *dGBA1b*$^{-/-}$ fly heads. There was a significant increase in β-GAL activity in older 25-d-old *dGBA1b*$^{-/-}$ fly heads compared with age-matched w^{1118} control flies. $^{***}p = 2 \times 10^{-5}$. Data are the mean ± SEM of three independent experiments. ***E***, The 25-d-old *dGBA1b*$^{-/-}$ and *dGBA1a,b*$^{-/-}$ flies had reduced whole-body levels of TAG compared with age-matched controls. $^{*}p = 0.046$ (paired *t* test). $^{***}p = 0.00082$ (paired *t* test). ***F***, Day 15 *dGBA1b*$^{-/-}$ and *dGBA1a,b*$^{-/-}$ flies were more sensitive to starvation conditions than age-matched w^{1118} control flies ($p = 3 \times 10^{-20}$ and $p = 5 \times 10^{-51}$; $n = 150$ flies per genotype). ***G***, Day 15 *dGBA1b*$^{-/-}$ flies had reduced feeding activity as assessed by the proboscis-extension assay ($n = 55$ flies per genotype). $^{*}p = 0.040$.

dGBA1b and the double-mutant *dGBA1a,b*$^{-/-}$ flies were almost completely infertile (Fig. 2*F*).

Knock-out of *dGBA* resulted in changes in lipid metabolism and accumulation of glucosylceramide

We next assessed whether knock-out of dGBA activity in the fly is associated with accumulation of its substrate, glucosylceramide. Indeed, using lipid mass spectrometry, we found that *dGBA1b*$^{-/-}$ and *dGBA1a,b*$^{-/-}$ flies displayed significant accumulation of glycosylceramide in their heads, whereas the heads of w^{1118} control flies contained very little glycosylceramide (Fig. 3*A*,*B*). Furthermore, the predominant glycosylceramide isoforms produced were C:16, C:18, and C:20 fatty chains (Fig. 3*A*,*B*). To determine whether loss of dGBA caused any change in the activity of other lysosomal enzymes, we also assessed hexosaminidase (Fig. 3*C*) and β-galactosidase (Fig. 3*D*). There was no age-dependent decrease in the activity of these two enzymes in the heads of *dGBA1b*$^{-/-}$ flies compared with controls. Indeed, the activity of β-galactosidase in day 25 *dGBA1b*$^{-/-}$ fly heads was significantly higher than in the controls (Fig. 3*D*).

In addition to specific lipid defects caused by the loss of dGBA we also looked at more general lipid abnormalities. As mentioned above, *dGBA1* is expressed in both the midgut and the fat body of the fly, an organ analog of vertebrate adipose tissue and liver that acts as a major organ of energy metabolism and nutrient storage (Tatar et al., 2014). We therefore assessed whether loss of dGBA in these tissues might result in general defects in lipid metabolism. TAG is the main form of lipid storage in the fly and therefore reflects the ability of flies to respond to starvation conditions (Ballard et al., 2008). Measurement of whole-body TAG levels in day 25 female flies revealed a significant reduction in *dGBA* knock-out flies compared with age-matched controls (Fig. 3*E*). In particular, there was a greater reduction in TAG levels in double-mutant *dGBA1a,b*$^{-/-}$ flies compared with the single-mutant *dGBA1b*$^{-/-}$ flies (Fig. 3*E*). The physiological relevance of the decrease in TAG levels was confirmed in both *dGBA1b*$^{-/-}$ and, to a greater extent, in *dGBA1a,b*$^{-/-}$ flies, which were more sensitive to starvation conditions compared with controls (Fig. 3*F*). Furthermore, assessment of feeding behavior by measuring proboscis-extension (Wong et al., 2009) demonstrated that *dGBA1b*$^{-/-}$ flies had significantly reduced feeding activity compared with controls (Fig. 3*G*). This suggests that reduced food intake may contribute to the reduced TAG levels and hypersensitivity to starvation.

Loss of dGBA activity led to lysosomal-autophagic deficits

To determine whether the accumulation of the dGBA substrate corresponds with abnormal lysosomal pathology, which is characteristic of GD, we stained the brains of *dGBA1b*$^{-/-}$ and *dGBA1a,b*$^{-/-}$ flies with LysoTracker and visualized the lysosomes with confocal microscopy. Aged *dGBA1b*$^{-/-}$ and *dGBA1a,b*$^{-/-}$ flies displayed numerous enlarged and abnormal lysosomes in their brains, which were not seen in age-matched control brains (Fig. 4*A*,*B*). Given that normal lysosomes are required to fuse with autophagosomes to form autophagolysosomes in the process of autophagy (Rubinsztein et al., 2012), we next studied autophagy. During the elongation phase, the cytosolic form of protein microtubule-associated protein 1 light chain 3 (LC3), LC3-I, is conjugated to phosphatidylethanolamine to form LC3-II, which is specifically targeted to the autophagosome membrane, where it remains until fusion with lysosomes. LC3 is therefore considered a good marker for studying autophagy (Ravikumar et al., 2010). We therefore measured the accumulation of Atg8, the fly ortholog of LC3, in both the heads of *dGBA1b*$^{-/-}$ and headless bodies of *dGBA1a,b*$^{-/-}$ flies, respectively (Fig. 5*A*,*B*). Western blot analysis demonstrated that Atg8-I and Atg8-II accumulated in the heads of flies lacking *dGBA1b*$^{-/-}$ (Fig. 5*A*). Atg8-II also accumulated in the headless bodies of flies lacking both *dGBA1* genes (*dGBA1a,b*$^{-/-}$) (Fig. 5*B*) compared with controls. Increased steady-state levels of Atg8-II suggests increased autophagosome number, but the marked increase in Atg8-I also could indicate a stall in flux activity in the brains of *dGBA1b*$^{-/-}$ flies (Fig. 5*A*). Analysis of the Atg8-II/Atg8-I ratio also confirmed increased autophagosome formation and autophagy block in the dGBA knock-out fly heads and bodies (Fig. 5*A*,*B*). Furthermore, Atg8 levels in homogenates of heads from control and *dGBA1b*$^{-/-}$ mutant flies demonstrated that this tissue was unresponsive to nutrient deprivation (Fig. 5*A*), unlike headless bodies, in which a brief 48 h period of prior starvation slightly increased Atg8-II levels, suggestive of autophagy induction (Fig. 5*B*).

p62 and polyubiquitinated proteins accumulated in dGBA-deficient fly brains

To study the downstream effects of autophagic dysfunction, we next performed immunostaining on the brains of dGBA-deficient flies with antibodies against ubiquitin and p62, markers of lysosomal-autophagic degradation (Bartlett et al., 2011). Under normal physiological conditions, p62 can link ubiquitinated proteins to the autophagy machinery (e.g., Atg8-II), targeting them for degradation (Rogov et al., 2014). Moreover, both ubiquitin and p62 accumulate when autophagy is inhibited (Bartlett et al., 2011) and are abundant constituents of protein inclusions associated with neurological diseases, including LBs in PD (Zatloukal et al., 2002; Bartlett et al., 2011). We first dissected *Drosophila* brains and visualized these proteins using antibodies against polyubiquitinated proteins and the fly ortholog of p62, Ref(2)P. Aged *dGBA1b*$^{-/-}$ brains displayed elevated levels of both ubiquitinated proteins and p62/Ref(2)P-containing aggregates under the confocal microscope, which were not seen in age-matched control fly brains (Fig. 6*A*). We also confirmed elevated levels of polyubiquitinated proteins in *dGBA1b*$^{-/-}$ fly heads using Western blot analysis (Fig. 6*B*). Thus, dGBA knock-out led to lysosomal-autophagic defects and the accumulation of ubiquitin and p62/Ref(2)P-containing deposits in the fly brain.

Knock-out of dGBA in the fly brain led to synaptic loss and neurodegeneration

To study the effect of dGBA deficiency on synaptic viability, we performed immunostaining for Bruchpilot, an essential component of synaptic active zones in *Drosophila* (Wagh et al., 2006). This revealed significantly reduced Bruchpilot in the brains of *dGBA1b*$^{-/-}$ flies compared with controls, suggesting synaptic loss (Fig. 7*A*).

We also performed an ultrastructural examination of *dGBA1b*$^{-/-}$ fly brains using transmission electron microscopy. This demonstrated grossly abnormal morphology of the ommatidia, the units of the compound eye, in *dGBA1b*$^{-/-}$ flies compared with controls (Fig. 7*B*). Quantitative analysis showed that the average rhabdomere area within each ommatidium was significantly reduced in the eyes of *dGBA1b*$^{-/-}$ flies (Fig. 7*B*).

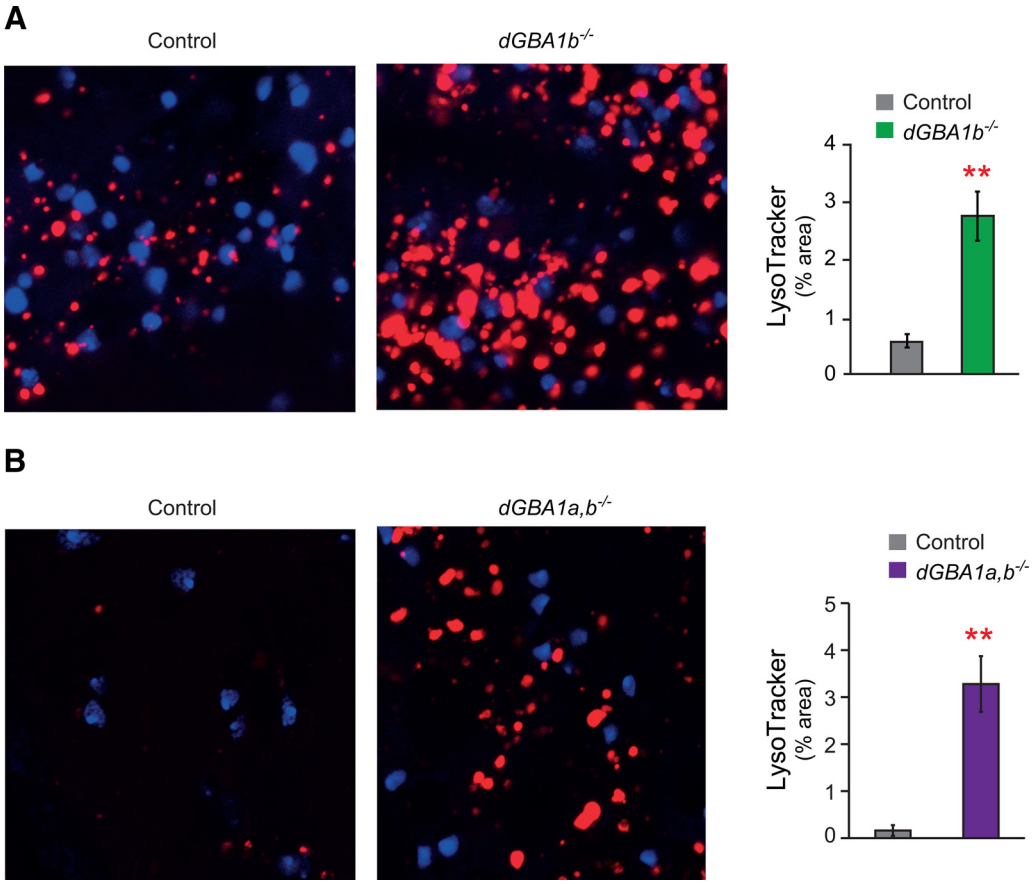

Figure 4. dGBA deficiency was associated with lysosomal defects. ***A***, Brains dissected from 15-d-old w^{1118} control or $dGBA1b^{-/-}$ flies were stained with LysoTracker and imaged live within 15 min of dissection, using the same microscope settings to capture images from the same region of the subesophageal ganglion in each brain. $dGBA1b^{-/-}$ flies displayed abnormal staining with numerous enlarged lysosomes that were not seen in age-matched control flies. For each image, the area of LysoTracker staining above a uniform threshold was quantified, revealing a significantly increased area of LysoTracker staining in $dGBA1a,b^{-/-}$ flies ($n = 6$ experiments with one control and one $dGBA1b^{-/-}$ brain in each experiment). $^{**}p < 0.005$ (paired t test). ***B***, Similar results were also seen in the brains of 25-d-old $dGBA1a,b^{-/-}$ flies compared with age-matched control flies ($n = 6$ experiments with one control and one $dGBA1a,b^{-/-}$ brain in each experiment). $^{**}p < 0.005$ (paired t test).

Knock-out of d*GBA* in the brain was associated with mitochondrial abnormalities and hypersensitivity to oxidative stress

Ultrastructural examination of the brains of flies lacking dGBA using electron microscopy revealed giant mitochondria in day 25 $dGBA1b^{-/-}$ fly brains compared with age-matched controls (Fig. 8*A*) or younger day 5 $dGBA1b^{-/-}$ brains (data not shown), with an ~25% increase in the average mitochondrial area (Fig. 8*B*). The presence of giant mitochondria, in addition to the increase in autophagy substrates and increased Atg8-II, further supported the conclusion that there was impaired autophagic flux.

In keeping with our ultrastructural data, mitochondrial dysfunction has been shown in a mouse model of GBA deficiency (Osellame et al., 2013) and GD human fibroblasts (de la Mata et al., 2015). To assess mitochondrial function, we measured ATP levels and found that they were reduced by ~40% in the brains of $dGBA1b^{-/-}$ flies as well as in the whole bodies of $dGBA1b^{-/-}$ and $dGBA1a,b^{-/-}$ flies compared with controls (Fig. 8*C*,*D*). Mitochondrial dysfunction can lead to decreased resistance to reactive oxygen species, which has been implicated in many neurodegenerative diseases (Kinghorn et al., 2015). To explore the role of d*GBA* in resistance to oxidative stress, we examined the survival of *dGBA*-deficient flies after exposure to the potent oxidizer hydrogen peroxide (H_2O_2) and paraquat, a free radical generator. Consistent with the mitochondrial abnormalities in aged flies, day 15 $dGBA1b^{-/-}$ and $dGBA1a,b^{-/-}$ flies showed increased sensitivity to H_2O_2 and paraquat stress (Fig. 8*E*,*F*).

Targeting downstream autophagy defects with the mTOR inhibitor rapamycin

The nutrient-sensing mTOR pathway regulates lysosomal biogenesis and autophagy (Ravikumar et al., 2010). We hence assessed the activity of mTOR by measuring the phosphorylation level of S6K, which acts downstream of mTOR complex 1 (mTORC1) (Castillo-Quan et al., 2015). Western blot analysis revealed a decrease in S6K phosphorylation in the heads of $dGBA1b^{-/-}$ flies compared with controls, indicating downregulation of mTORC1 (Fig. 9*A*), which would be predicted to lead to an increase in autophagy. We also tested whether rapamycin, a known mTORC1 inhibitor (Bjedov et al., 2010), could further downregulate mTOR in dGBA-deficient flies. Treatment of control flies with 200 μM rapamycin resulted in a >50% decrease in S6K phosphorylation. There was a trend for rapamycin treatment of $dGBA1b^{-/-}$ flies to further decrease S6K phosphorylation, although this was not statistically significant. We therefore tested the effect of rapamycin on the lifespan of $dGBA1b^{-/-}$ flies. Interestingly, we found that rapamycin supplementation to the fly medium (both 200 and 400 μM) from 2 d of age was able to partially ameliorate the lifespan defect in $dGBA1b^{-/-}$ flies (Fig. 9*B*). Consistent with previous work (Bjedov et al., 2010), rapa-

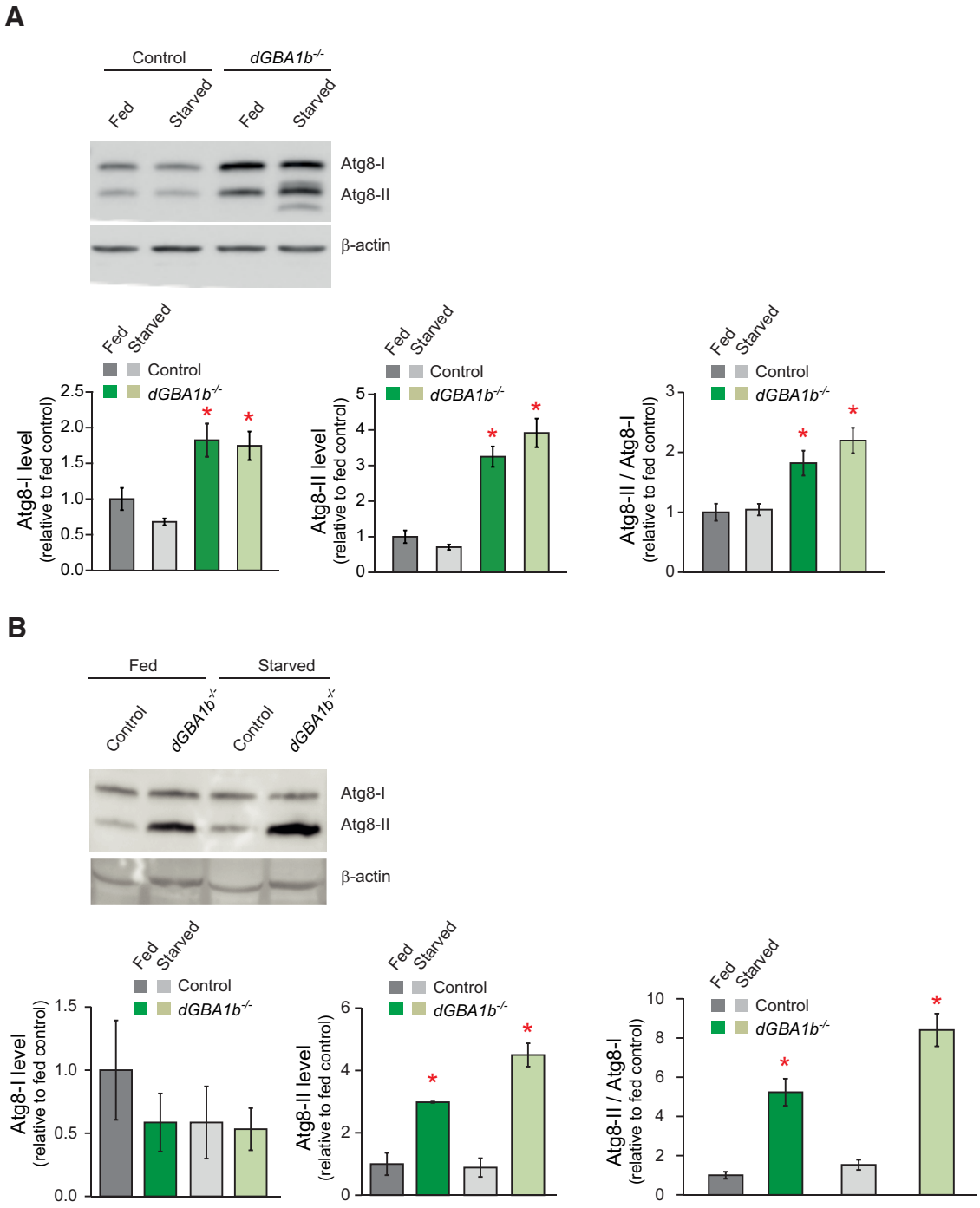

Figure 5. Flies lacking dGBA displayed a block in autophagy. ***A***, Western blot analysis with an antibody against the fly LC 3 ortholog, Atg8, demonstrated increased levels in *dGBA1b*$^{-/-}$ fly heads compared with age-matched w^{1118} control flies. Both Atg8-I and Atg8-II were increased compared with controls, and the ratio of Atg8-II/Atg8-I in *dGBA1b*$^{-/-}$ flies indicated increased autophagosome formation ($n = 3$ experiments). *$p < 0.05$. ***B***, Western blot analysis of Atg8 levels in the headless bodies of *dGBA1a,b*$^{-/-}$ flies demonstrated no significant change in Atg8-I levels, with an increase in Atg8-II levels and an increased Atg8-II/Atg8-I ratio. This effect was more pronounced after starvation in *dGBA1a,b*$^{-/-}$ flies ($n = 3$ experiments). *$p < 0.05$.

mycin also increased the lifespan of control flies (Fig. 9*B*). In keeping with the effect on lifespan, 400 μM rapamycin, but not 200 μM (data not shown), was also able to partially rescue the locomotor deficits in aged *dGBA1b*$^{-/-}$ flies (Fig. 9*C*). An even greater rescue was seen in flies lacking both *dGBA1* genes (*dGBA1a,b*$^{-/-}$). This effect of rapamycin appeared to be specific to dGBA knock-out flies, as rapamycin did not have a significant effect on the climbing ability of age-matched control flies (Fig. 9*C*). We also assessed the effect of rapamycin on the response to oxidative stress. Treatment with 200 μM rapamycin from 2 to 15 d of age subsequently prolonged the survival of *dGBA1b*$^{-/-}$ flies on food containing H_2O_2 (Fig. 9*D*). This effect was also specific to dGBA-deficient flies, as surprisingly rapamycin-treated control flies had reduced lifespan on exposure to H_2O_2 (Fig. 9*D*).

Rapamycin treatment is also associated with an increased resistance to starvation in wild-type flies (Bjedov et al., 2010). We therefore treated *dGBA1b*$^{-/-}$ flies with rapamycin for the

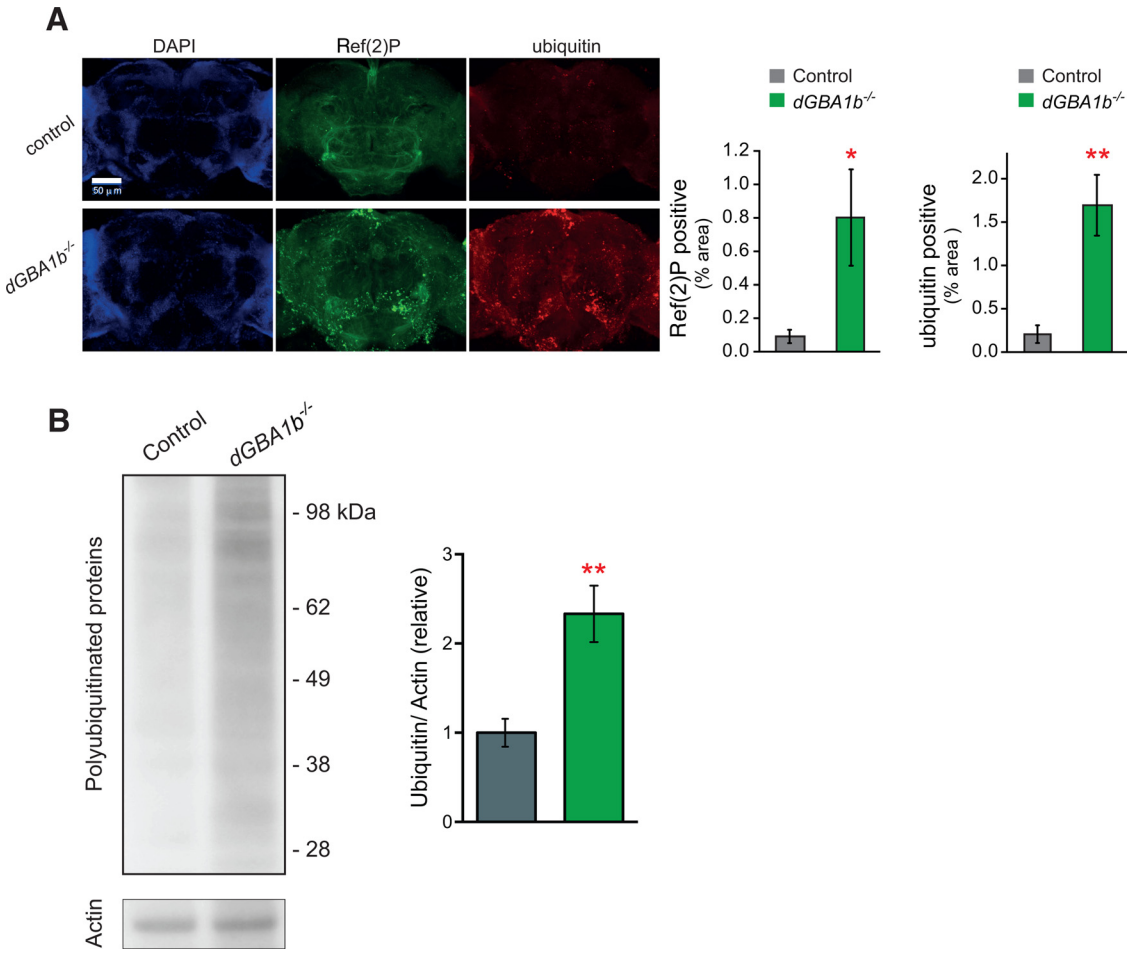

Figure 6. dGBA-deficient flies showed accumulation of p62/Ref(2)P and polyubiquitinated proteins in their brains. ***A***, Immunostaining with antibodies against Ref(2)P, the fly ortholog of p62, and polyubiquitinated proteins demonstrated increased Ref(2)P- and ubiquitin-positive puncta within the $dGBA1b^{-/-}$ fly brains. $^{*}p < 0.05$ (*t* test). $^{**}p < 0.001$ (*t* test). $n = 5$ or 6 brains per genotype. ***B***, Western blotting of Triton-insoluble head extracts confirmed the presence of significantly increased levels of polyubiquitinated proteins in $dGBA1b^{-/-}$ flies. $^{**}p < 0.05$. $n = 4$ samples per genotype, 10–15 heads per sample.

first 15 d of adulthood before exposing them to starvation conditions. The 200 μM rapamycin was able to rescue the survival of $dGBA1b^{-/-}$ flies and control flies under starvation conditions (Fig. 9*E*). These findings suggest that, despite the autophagy block in flies lacking dGBA, rapamycin is still able to exert protective effects on lifespan, locomotor defects, and oxidative and starvation stress responses, likely by exerting a small but functionally significant increase in mTOR inhibition.

Loss of dGBA function in the brain resulted in an upregulation of *Mitf* gene expression and its downstream target gene *Atg8a*

To further study the effects of dGBA deficiency and rapamycin treatment on autophagy, we measured the expression levels of *Mitf* and its downstream target *Atg8a*. *Mitf* is the fly ortholog of the mammalian transcription factor EB (*TFEB*) gene, the master regulator of lysosomal biogenesis and autophagy (Bouché et al., 2016; Tognon et al., 2016). *TFEB* is critical for the autophagic cellular clearance of abnormal proteins and organelles, as well as lipid metabolism. *TFEB* acts by coordinating the expression of a number of genes belonging to the Coordinated Lysosomal Expression and Regulation (CLEAR) network, by directing binding to specific CLEAR-box sequences located near their promoters. *TFEB* is usually cytosolic where it interacts with mTORC1 at the surface of the lysosome (Roczniak-Ferguson et al., 2012), but during starvation it translocates to the nucleus where it induces target gene transcription. Studies have shown that *Mitf* has conserved regulatory mechanisms with mammalian TFEB, translocating to the nucleus when *Drosophila* mTORC1 is inhibited (Bouché et al., 2016).

We first measured *Mitf* gene expression in the heads of $dGBA1b^{-/-}$ flies. qRT-PCR data analysis showed that, in response to the loss of dGBA activity in the brain, there is a highly significant upregulation of *Mitf* gene expression (Fig. 10*A*). We next studied the levels of the *Atg8a* gene, the fly ortholog of the mammalian *GABARAPL1* gene, which acts downstream of *Mitf*. This gene is involved in the main steps of autophagosome formation and maturation. In keeping with the upregulation of *Mitf* in $dGBA1b^{-/-}$ fly heads, *Atg8a* was also upregulated in response to dGBA knockdown in the fly brain (Fig. 10*B*).

We also studied the effect on *Mitf* and *Atg8a* gene expression of treating dGBA-deficient and control flies with 200 μM rapamycin from day 2 (Fig. 10*A*,*B*). Interestingly, we did not see any increase in *Mitf* gene expression in $dGBA1b^{-/-}$ flies treated with rapamycin compared with untreated flies (Fig. 10*A*). Moreover, the levels of *Atg8a* in rapamycin-treated $dGBA1b^{-/-}$ flies were significantly downregulated compared with untreated flies (Fig. 10*B*). Rapamycin significantly increased the expression levels of *Mitf* in control flies (Fig. 10*A*); and although there was a trend

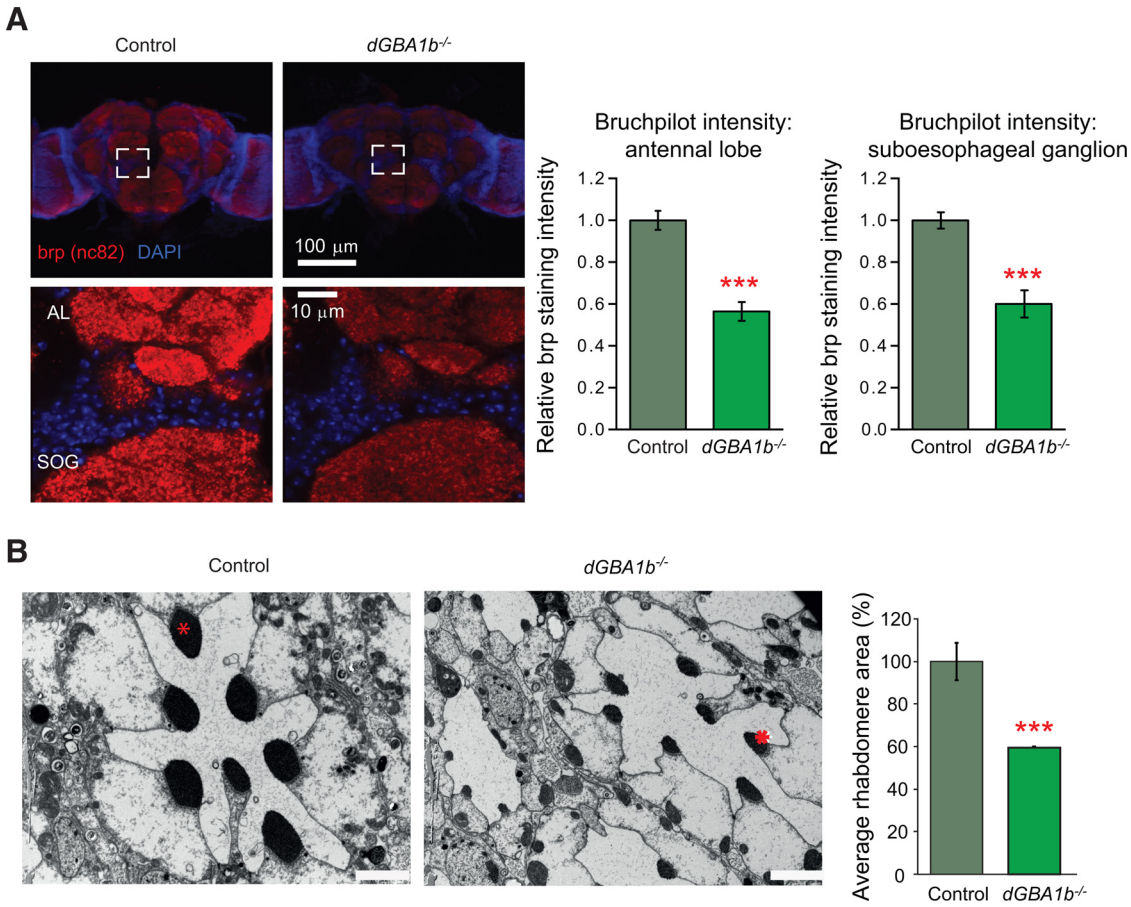

Figure 7. Deficiency of dGBA resulted in synaptic loss and neurodegeneration. ***A***, Immunostaining for Bruchpilot (brp), a critical synaptic component, demonstrated reduced staining (red) in the brains of day 25 *dGBA1b*$^{-/-}$ flies compared with controls. Antennal lobe (AL) and suboesphageal (SOG). $n = 7–8$ brains per genotype. ***B***, EM of the eyes of day 25 *dGBA1b*$^{-/-}$ flies revealed grossly abnormal morphology of the ommatidia compared with age-matched controls (×5600). Scale bars, 2 μm. In addition, quantitative analysis revealed a reduction in average rhabdomere (*) area in *dGBA1b*$^{-/-}$ fly eyes (***$p = 4 \times 10^{-6}$; at least 80 consecutive rhabdomeres studied for each genotype).

toward increasing *Atg8a* levels, it was not statistically significant (Fig. 10*B*). Thus, loss of dGBA activity in the brain is associated with increased expression levels of *Mitf*, and its downstream target gene, *Atg8a*, but upregulation of *Mitf* expression is not responsible for the protective effect of rapamycin on lifespan, locomotor, and oxidative stress phenotypes.

Discussion

We generated a *Drosophila* model of neuronopathic GD. Simple genetics could not be used to precisely excise both *Drosophila GBA1* genes, *dGBA1a* and *dGBA1b,* due to the presence of the CG31413 gene between them. Therefore, we used serial homologous recombination to knock out both *dGBA1* genes separately or together in the fly. Of the two fly GBA orthologs, only *dGBA1b* is expressed in the fly brain (Flyatlas). *dGBA1b*$^{-/-}$ fly heads, lacking dGBA1b expression, displayed accumulation of the dGBA substrate glucosylceramide. Furthermore, the glucosylceramide isoforms (C16:0, C18:0, C22:0) were similar to those found in human spleen tissue (with the addition of hydroxylated or longer chain isoforms including C18:0-OH, C20:0-OH, C24:1, and C24:0 in the human tissue (N. Sebire and S. Paine, unpublished data). Moreover, this is consistent with data showing accumulation of glucosylceramide and glucosylsyphingosine in Types II and III GD patient brains (Orvisky et al., 2002).

Abnormally engorged lysosomes in *dGBA1b*$^{-/-}$ fly brains were visualized with LysoTracker, confirming the validity of this neuronopathic GD fly model. Lysosomal integrity is necessary for normal functioning of the autophagy degradation machinery (Xu and Ren, 2015), and accordingly we observed autophagy dysfunction in *dGBA1b*$^{-/-}$ brains, with accumulation of the autophagolysosomal protein Atg8/LC3. Thus, we demonstrate autophagy defects at the level of the autophagic machinery *in vivo* in a GD *Drosophila* model, following on from *in vitro* studies in GD macrophages and iPSCs showing impaired autophagy (Awad et al., 2015; Aflaki et al., 2016; Fernandes et al., 2016).

Neuronal-specific autophagy deficits, through loss of the mouse autophagy genes *atg7* or *atg5*, result in accumulation of polyubiquitinated proteins, behavioral defects, and reduced longevity (Hara et al., 2006; Komatsu et al., 2006). Consistent with this, we found that *dGBA1b*$^{-/-}$ flies displayed reduced survival and locomotor ability and brain accumulation of p62/Ref(2)P and polyubiquitinated proteins. Both p62 and ubiquitin accumulate in neurodegenerative diseases, such as Alzheimer's disease and PD (Zatloukal et al., 2002; Bartlett et al., 2011), and multiple pathogenic proteins, including p62 and β-amyloid, have been identified in neuronopathic GD mouse brains (Xu et al., 2014).

Surprisingly, knock-out of *dGBA1a*, which is predominantly expressed in the digestive system, significantly increased survival. This finding parallels recent research in *Drosophila* and *Caenorhabditis elegans* demonstrating that the intestine is an important target organ for mediating lifespan extension at the organismal

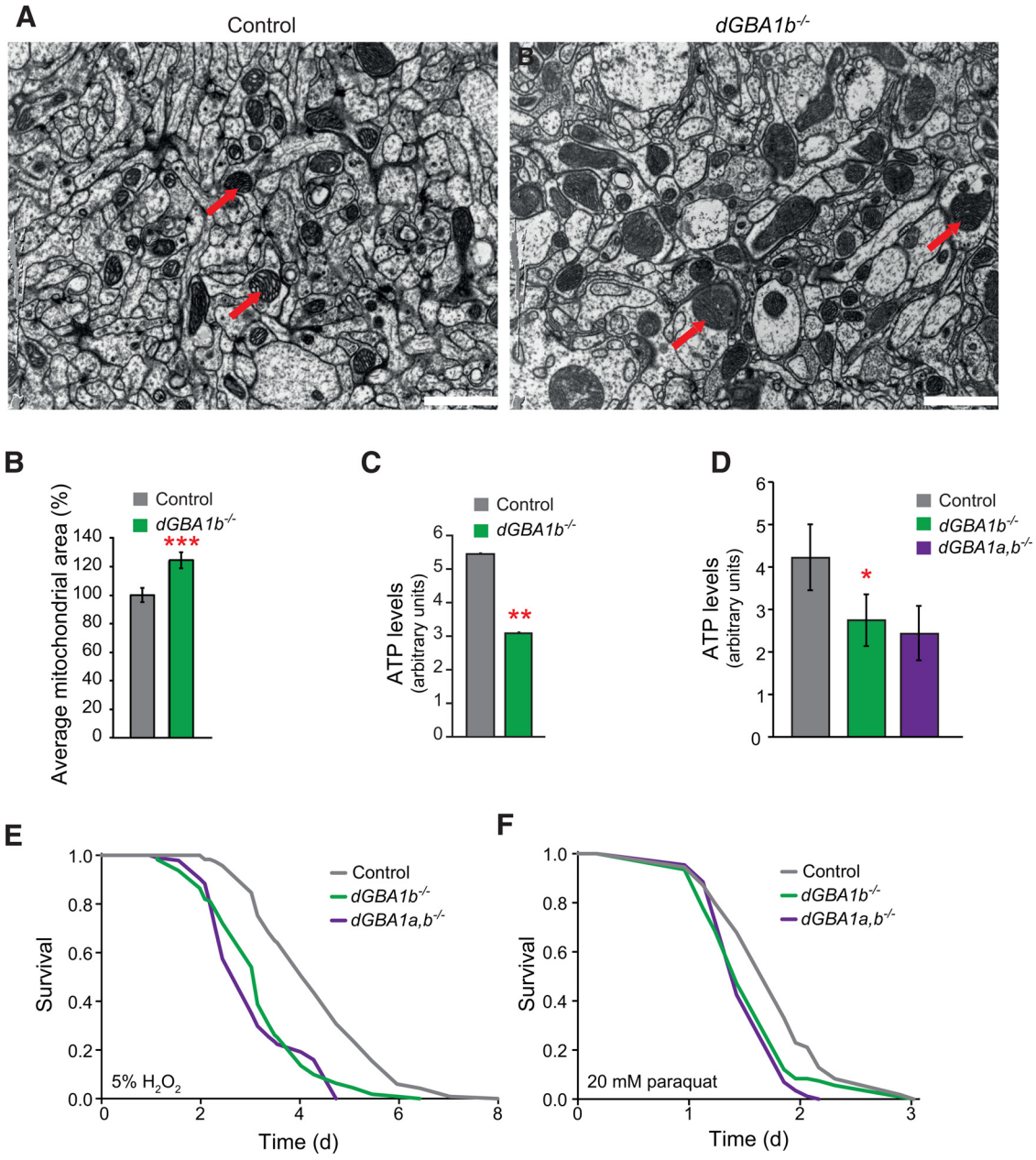

Figure 8. dGBA-deficient fly brains displayed mitochondrial abnormalities. ***A***, EM analysis of the brains of day 25 $dGBA1b^{-/-}$ flies showed giant mitochondria (arrows) compared with mitochondria (arrows) in age-matched w^{1118} control fly brains (×11,500 magnification). Scale bar, 1 μm. ***B***, Average mitochondrial area was increased in $dGBA1b^{-/-}$ flies ($n > 200$ mitochondria per genotype). $^{***}p = 4 \times 10^{-5}$. ***C***, These mitochondrial structural abnormalities were associated with decreased ATP levels in day 25 $dGBA1b^{-/-}$ fly heads ($^{**}p = 0.0016$) and (***D***) in the whole bodies of $dGBA1b^{-/-}$ flies compared with age-matched controls ($^{*}p = 0.02$). There was a trend for reduced ATP levels in the $dGBA1a,b^{-/-}$ flies, but this did not quite reach significance ($p = 0.06$). ***E***, $dGBA1b^{-/-}$ and $dGBA1a,b^{-/-}$ flies displayed reduced survival on exposure to 5% H_2O_2 ($p = 3 \times 10^{-12}$ and $p = 5 \times 10^{-15}$) and (***F***) 20 mM paraquat ($p = 0.003$ and $p = 2 \times 10^{-6}$; $n = 150$ flies per genotype).

level, with single-gene manipulations specifically in the gut prolonging lifespan (Rera et al., 2011; Tatar et al., 2014). The role of dGBA in the gut in regulating lifespan was beyond the scope of this study but is an area that warrants further investigation. We demonstrated, however, that the lifespan extension seen in $dGBA1a^{-/-}$ flies is not associated with any improvement in locomotor ability.

Mitochondrial integrity is necessary for normal autophagy-lysosomal system functioning (Palikaras and Tavernarakis, 2012; Ashrafi and Schwarz, 2013). Indeed, mitochondrial dysfunction occurs in GD mouse models (Osellame et al., 2013; Xu et al., 2014), likely due to defects in the autophagic removal of damaged mitochondria (Osellame et al., 2013). In keeping with this, the deficiency of the *Drosophila* autophagy gene *atg7* is associated with sensitivity to oxidative stressors (Juhász et al., 2007). Accordingly, we demonstrated mitochondrial abnormalities in $dGBA1b^{-/-}$ flies, with giant mitochondria, reduced ATP and hypersensitivity to oxidative stress. Enlarged mitochondria and decreased ATP occur in neuronopathic GD mice (Xu et al., 2014), and giant mitochondria are directly linked to *Drosophila* autophagy defects (Bouché et al., 2016). Therefore, the accumulation of autophagic substrates and giant mitochondria in $dGBA1b^{-/-}$ flies is consistent with autophagy block (Fig. 10*C*).

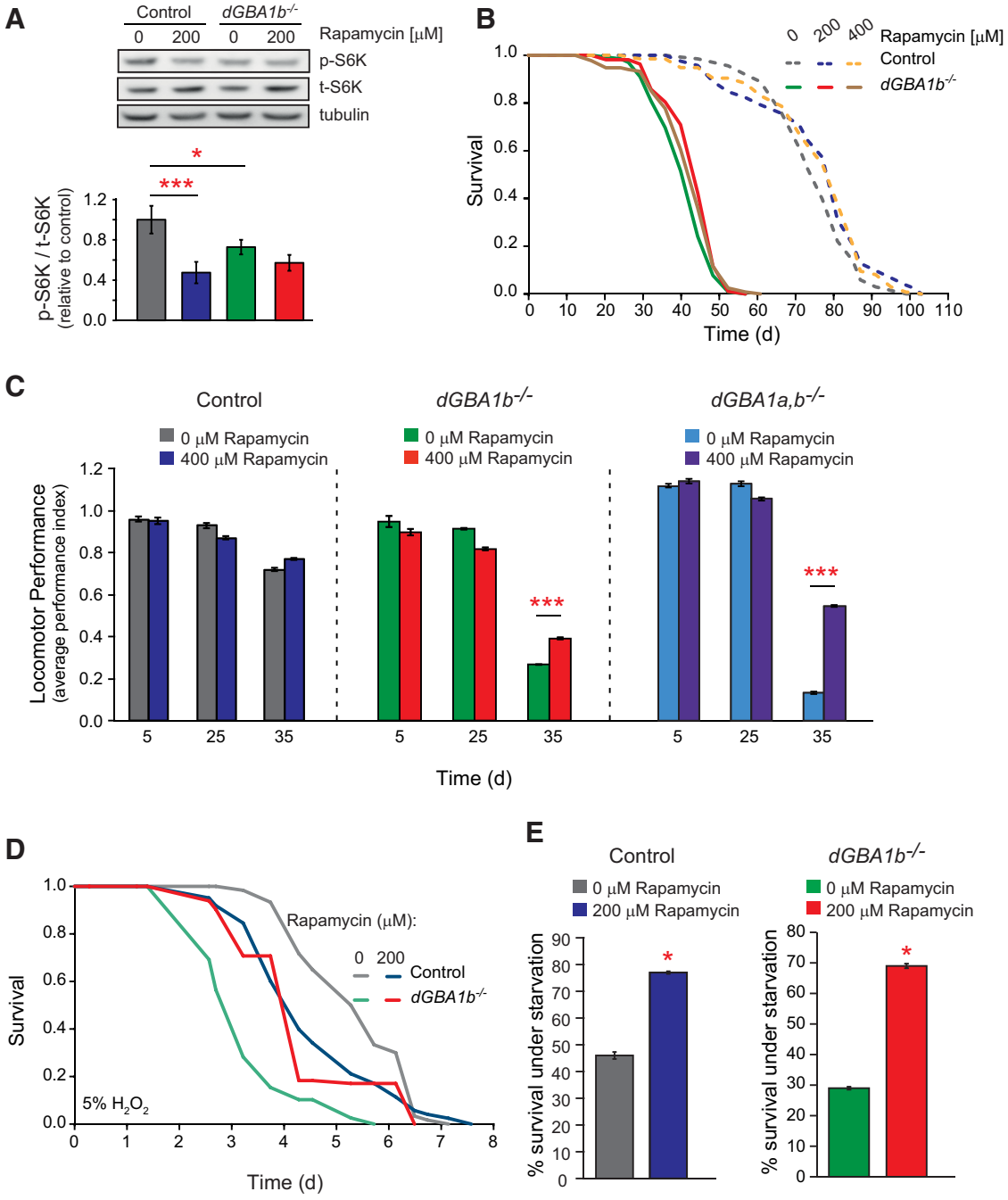

Figure 9. The mTOR inhibitor rapamycin partially ameliorated the lifespan, locomotor, oxidative stress, and starvation phenotypes in dGBA-deficient flies. ***A***, Day 7 *dGBA1b*$^{-/-}$ fly heads had significantly decreased phosphorylated S6K (p-S6K) levels compared with age-matched control flies. *$p = 0.0414$. Treatment of control flies with 200 μM rapamycin led to a reduction in phospho-S6K levels. ***$p = 0.0009$. Although there was a trend for rapamycin to further decrease phospho-S6K levels in *dGBA1b*$^{-/-}$ flies, this was not statistically significant ($p = 0.327$, one-way ANOVA with Bonferroni correction). ***B***, The 200 and 400 μM of rapamycin significantly extended the lifespan of *dGBA1b*$^{-/-}$ flies ($p = 0.005$ and $p < 0.05$; $n = 110–160$ flies per genotype and condition). As previously demonstrated, rapamycin also extended the lifespan of w^{1118} control flies ($p = 0.007$ and $p = 0.02$). ***C***, Treatment with 400 μM rapamycin partially rescued the age-related climbing defects in day 35 *dGBA1b*$^{-/-}$ flies and *dGBA1a,b*$^{-/-}$ flies (***$p = 0.0005$ and ***$p = 0.0006$), but did not have a significant effect on the climbing ability of age-matched control flies ($p = 0.23$; $n = 45$ flies per genotype and condition, average of 3 repeats). ***D***, Treatment of *dGBA1b*$^{-/-}$ flies from 2 to 15 d of age with 200 μM rapamycin partially rescued the survival on subsequent exposure to food containing 5% H_2O_2 ($p = 2.5 \times 10^{-9}$). This protective effect was specific to dGBA-deficient flies as 200 μM rapamycin was toxic to control flies under similar conditions ($p = 0.0007$; $n = 60$ flies per group). ***E***, The 200 μM rapamycin was also able to increase survival of *dGBA1b*$^{-/-}$ flies in response to subsequent exposure to starvation conditions from 15 d of age. *$p = 0.004$. The time point shown is after 3 d of starvation stress ($n = 60$ flies per condition). Under similar conditions, 200 μM rapamycin also rescued the survival of control w^{1118} flies ($n = 60$ flies per group). *$p = 0.023$. The bar chart represents survival after 8 d of exposure to starvation.

Furthermore, we demonstrated that the neuropathological defects in *dGBA1b*$^{-/-}$ flies occur independently of α-synuclein, confirming that dGBA deficiency is sufficient to cause neurodegeneration (Fig. 10*C*). A recent study using a deletion mutant harboring imprecise removal of the *dGBA1b* gene, as well as the incomplete removal of the *dGBA1a* gene and excision of the interjacent *CG31413* gene, provides further validation of our model for studying *GBA1*-associated neurodegeneration. Loss of 60% of GCase activity was also associated with reduced survival and climbing ability in addition to accumulation of autophagy sub-

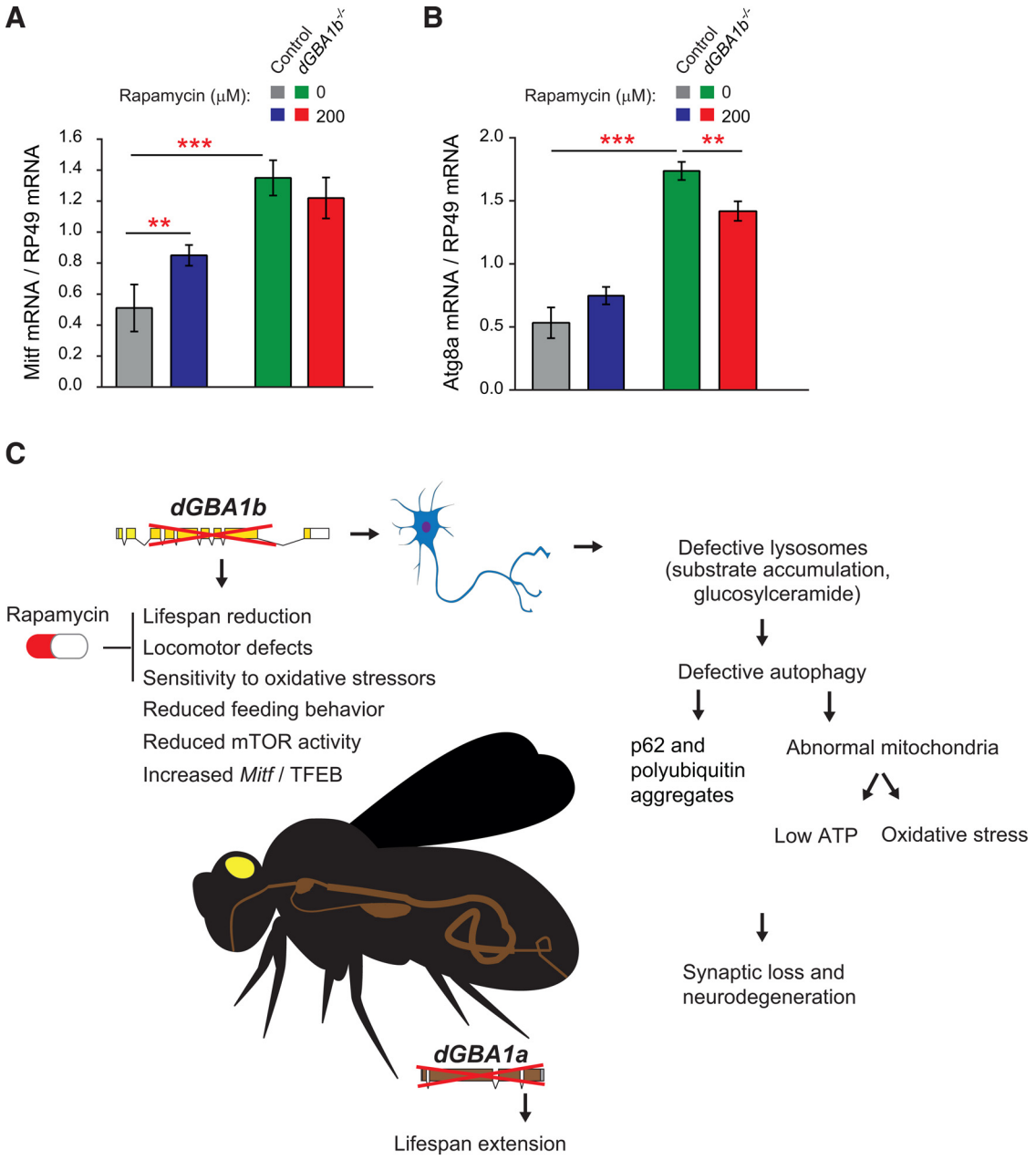

Figure 10. Knock-out of dGBA activity in the fly brain was associated with upregulation of *Mitf* and its downstream target *Atg8a*. ***A***, qRT-PCR data analysis revealed that day 15 $dGBA1b^{-/-}$ fly heads had increased expression levels of *Mitf* compared with controls. $^{***}p = 9.7 \times 10^{-5}$. In addition, treatment with 200 μM rapamycin from 2 d of age had no significant effect on *Mitf* gene expression in $dGBA1b^{-/-}$ flies ($p = 0.32$). However, rapamycin treatment led to a significant increase in the expression levels of *Mitf* in control flies ($^{**}p = 0.016$). ***B***, *Atg8a* gene expression levels were greater in $dGBA1b^{-/-}$ fly heads compared with controls. $^{***}p = 2.8 \times 10^{-7}$. Treatment with 200 μM rapamycin resulted in a decrease in *Atg8a* gene levels in $dGBA1b^{-/-}$ fly heads ($^{**}p = 0.002$); and although there was a trend toward increased *Atg8a* gene expression in control flies with rapamycin treatment, it did not reach statistical significance ($p = 0.054$). The mRNA expression levels of all genes are shown relative to the expression levels of a control gene, *RP49*. ***C***, Schematic diagram showing the downstream effects of impaired autophagy flux in dGBA-deficient flies.

strates (Davis et al., 2016). GCase deficiency was also shown to enhance α-synuclein pathology in the fly (Suzuki et al., 2015; Davis et al., 2016). Our model has the advantage over existing models, as it allows the precise and complete knock-out of each of the *dGBA* genes, and the dissection of the role of dGBA in different tissues. The ability to knock out only brain-specific *dGBA1b* is particularly relevant given our finding that loss of *dGBA* in the gut causes prolongevity effects. Our model also avoids the production of truncated, possibly pathogenic, variants of *dGBA*.

The nutrient-sensing mTOR is localized to the lysosomal surface (Efeyan et al., 2012; Betz and Hall, 2013), where it modulates autophagy (Yu et al., 2010; Zoncu et al., 2011). It has thus been speculated that abnormal lysosomal function leads to activation of autophagy by mTOR downregulation (Li et al., 2013). Indeed, a recent study reported increased expression of mTOR signaling pathway genes in neuronopathic GD mice (Dasgupta et al., 2015). In view of the autophagy defect in $dGBA1b^{-/-}$ flies, we probed mTOR signaling by analyzing S6K phosphorylation downstream of mTORC1. Interestingly, we detected a decrease in S6K phosphorylation and hence downregulation of mTORC1 compared with controls. Furthermore, although not statistically significant, there was a trend for mTOR to be further downregulated in $dGBA1b^{-/-}$ flies treated with rapamycin, a known mTORC1 inhibitor. Because rapamycin has protective effects in animal

models of PD and other neurodegenerative diseases (Malagelada et al., 2010; Cheng et al., 2015), we treated *dGBA1b*$^{-/-}$ flies with rapamycin and found that, despite the autophagy block, it was able to partially ameliorate many neurotoxic phenotypes. Rapamycin treatment led to an improvement in the lifespan and climbing phenotypes, in addition to the hypersensitivity to oxidative and starvation stressors seen in *dGBA1b*$^{-/-}$ flies. These results are somewhat surprising given that rapamycin treatment of iPSC-derived neuronal cells from GD patients caused cell death (Awad et al., 2015), demonstrating that drug effects *in vitro* vary to those at the organismal level. Furthermore, although rapamycin increases the lifespan and protects against starvation conditions in control flies (Bjedov et al., 2010), the rescue of age-related climbing defects and oxidative stress appeared to be specific to dGBA-deficient flies. Indeed, rapamycin had no effect on the climbing ability of control flies, and rapamycin-treated control flies were more sensitive to H_2O_2 than untreated flies. The reason for the opposing effects of rapamycin on the oxidative stress responses of *dGBA1b*$^{-/-}$ and control flies is unclear, but may be related to the differential activation of oxidative stress pathways between *dGBA1b*$^{-/-}$ and healthy controls.

Lastly, we demonstrated that knock-out of dGBA in the brain results in an upregulation of *Mitf* and its downstream target, *Atg8a*, suggesting a compensatory response to the autophagy block. This is in contrast to findings in a recent study showing downregulation of *TFEB* expression in GD iPSC-derived cells (Awad et al., 2015). The reasons for these differing results is not clear, but possible explanations may relate to variations in autophagy block between models, and the fact that neuronal cells are newly differentiated and may reflect early disease compared with adult flies. *Mitf* gene expression may also vary in the presence of mutant dGBA. Our fly model displays very little dGBA expression compared with iPSC cells, which are derived from mutant carriers, and therefore, despite showing very low levels of GCase activity, express mutant GBA. Mutant GCase is known to exert gain-of-function toxic effects, including in *Drosophila*, with upregulation of the unfolded protein response (Maor et al., 2013, 2016). Knockdown of *Mitf* in *Drosophila* leads to similar phenotypes to those in *dGBA1b*$^{-/-}$ flies, including autophagy substrate accumulation, upregulation of Atg8-II, giant mitochondria, as well as enlarged lysosomes (Bouché et al., 2016). Thus, the autophagy defects seen in dGBA deficiency appear to phenocopy *Mitf* downregulation in the fly. This suggests that upregulating *Mitf* as a potential therapeutic strategy in GD and GBA-linked PD may be limited in its efficacy due to the inability of GBA-deficient neuronal tissue to stimulate autophagy. Further studies are warranted to explore the complex interaction between mTORC1 and *TFEB/Mitf* in GD.

Rapamycin treatment of *dGBA1b*$^{-/-}$ flies did not upregulate *Mitf* gene expression, suggesting that rapamycin does not act through *Mitf* signaling to rescue the neurotoxic phenotypes of dGBA-deficient flies. We hypothesize, therefore, that mTOR is downregulated in dGBA-deficient flies as a compensatory response to lysosomal-autophagy block. Possibly as a consequence of lysosomal dysfunction in dGBA-deficient flies, the normal interaction between mTORC1 and TFEB/Mitf at the surface of the lysosome is disrupted, leading to changes in *TFEB/Mitf* gene expression. Therefore, by exerting small additional effects on mTORC1 signaling, rapamycin may mediate its beneficial effects (Fig. 10*C*). Furthermore, *Mitf* also plays a critical role in lipid metabolism and recapitulates the function of *TFEB* in mammals in this regard (Bouché et al., 2016). *Mitf* expression may therefore contribute to the reduced TAG that we see in *dGBA1b*$^{-/-}$ flies.

In conclusion, the autophagy defects seen in our GD flies, likely as a result of failure of the fusion of autophagosomes and lysosomes, may also be relevant to PD linked to *GBA1* mutations. Our results raise the possibility that therapies aimed at ameliorating not only lysosomal dysfunction, but also at autophagic abnormalities, including lowering mTOR activity, may be effective in treating *GBA1*-associated disease. They also suggest that rapamycin may offer significant health benefits in neuronopathic GD and in *GBA1*-related synucleinopathies. Together, our data demonstrate that these *Drosophila* models of dGBA-deficiency are a useful platform to further study the downstream effects of lysosomal-autophagic dysfunction and to identify genetic modifiers and new therapeutic targets in neuronopathic GD and *GBA1*-associated PD.

References

Aflaki E, Moaven N, Borger DK, Lopez G, Westbroek W, Chae JJ, Marugan J, Patnaik S, Maniwang E, Gonzalez AN, Sidransky E (2016) Lysosomal storage and impaired autophagy lead to inflammasome activation in Gaucher macrophages. Aging Cell 15:77–88. CrossRef Medline

Ashrafi G, Schwarz TL (2013) The pathways of mitophagy for quality control and clearance of mitochondria. Cell Death Differ 20:31–42. CrossRef Medline

Auray-Blais C, Blais CM, Ramaswami U, Boutin M, Germain DP, Dyack S, Bodamer O, Pintos-Morell G, Clarke JT, Bichet DG, Warnock DG, Echevarria L, West ML, Lavoie P (2015) Urinary biomarker investigation in children with Fabry disease using tandem mass spectrometry. Clin Chim Acta 438:195–204. CrossRef Medline

Awad O, Sarkar C, Panicker LM, Miller D, Zeng X, Sgambato JA, Lipinski MM, Feldman RA (2015) Altered TFEB-mediated lysosomal biogenesis in Gaucher disease iPSC-derived neuronal cells. Hum Mol Genet 24:5775–5788. CrossRef Medline

Ballard JW, Melvin RG, Simpson SJ (2008) Starvation resistance is positively correlated with body lipid proportion in five wild caught *Drosophila simulans* populations. J Insect Physiol 54:1371–1376. CrossRef Medline

Bartlett BJ, Isakson P, Lewerenz J, Sanchez H, Kotzebue RW, Cumming RC, Harris GL, Nezis IP, Schubert DR, Simonsen A, Finley KD (2011) p62, Ref(2)P and ubiquitinated proteins are conserved markers of neuronal aging, aggregate formation and progressive autophagic defects. Autophagy 7:572–583. CrossRef Medline

Betz C, Hall MN (2013) Where is mTOR and what is it doing there? J Cell Biol 203:563–574. CrossRef Medline

Bjedov I, Toivonen JM, Kerr F, Slack C, Jacobson J, Foley A, Partridge L (2010) Mechanisms of life span extension by rapamycin in the fruit fly *Drosophila melanogaster*. Cell Metab 11:35–46. CrossRef Medline

Bouché V, Espinosa AP, Leone L, Sardiello M, Ballabio A, Botas J (2016) *Drosophila* Mitf regulates the V-ATPase and the lysosomal-autophagic pathway. Autophagy 12:484–498. CrossRef Medline

Castillo-Quan JI, Kinghorn KJ, Bjedov I (2015) Genetics and pharmacology of longevity: the road to therapeutics for healthy aging. Adv Genet 90:1–101. CrossRef Medline

Castillo-Quan JI, Li L, Kinghorn KJ, Ivanov DK, Tain LS, Slack C, Kerr F, Nespital T, Thornton J, Hardy J, Bjedov I, Partridge L (2016) Lithium promotes longevity through GSK3/NRF2-dependent hormesis. Cell Rep 15:638–650. CrossRef Medline

Cheng CW, Lin MJ, Shen CK (2015) Rapamycin alleviates pathogenesis of a new *Drosophila* model of ALS-TDP. J Neurogenet 29:59–68. CrossRef Medline

Cox TM (2010) Gaucher disease: clinical profile and therapeutic developments. Biologics 4:299–313. CrossRef Medline

Dasgupta N, Xu YH, Li R, Peng Y, Pandey MK, Tinch SL, Liou B, Inskeep V, Zhang W, Setchell KD, Keddache M, Grabowski GA, Sun Y (2015) Neuronopathic Gaucher disease: dysregulated mRNAs and miRNAs in brain pathogenesis and effects of pharmacologic chaperone treatment in a mouse model. Hum Mol Genet 24:7031–7048. CrossRef Medline

Davis MY, Trinh K, Thomas RE, Yu S, Germanos AA, Whitley BN, Sardi SP, Montine TJ, Pallanck LJ (2016) Glucocerebrosidase deficiency in *Drosophila* results in alpha-synuclein-independent protein aggregation and neurodegeneration. PLoS Genet 12:1–24. CrossRef Medline

de la Mata M, Cotán D, Oropesa-Ávila M, Garrido-Maraver J, Cordero MD,

Villanueva Paz M, Delgado Pavón A, Alcocer-Gómez E, de Lavera I, Ybot-González P, Paula Zaderenko A, Ortiz Mellet C, García Fernández JM, Sánchez-Alcázar JA (2015) Pharmacological chaperones and coenzyme Q10 treatment improves mutant β-glucocerebrosidase activity and mitochondrial function in neuronopathic forms of Gaucher disease. Sci Rep 5:10903. CrossRef Medline

Efeyan A, Zoncu R, Sabatini DM (2012) Amino acids and mTORC1: from lysosomes to disease. Trends Mol Med 18:524–533. CrossRef Medline

Fernandes HJ, Hartfield EM, Christian HC, Emmanoulidou E, Zheng Y, Booth H, Bogetofte H, Lang C, Ryan BJ, Sardi SP, Badger J, Vowles J, Evetts S, Tofaris GK, Vekrellis K, Talbot K, Hu MT, James W, Cowley SA, Wade-Martins R (2016) ER stress and autophagic perturbations lead to elevated extracellular α-synuclein in GBA-N370S Parkinson's iPSC-derived dopamine neurons. Stem Cell Rep 6:342–356. CrossRef Medline

Gong WJ, Golic KG (2004) Genomic deletions of the *Drosophila melanogaster* Hsp70 genes. Genetics 168:1467–1476. CrossRef Medline

Hara T, Nakamura K, Matsui M, Yamamoto A, Nakahara Y, Suzuki-Migishima R, Yokoyama M, Mishima K, Saito I, Okano H, Mizushima N (2006) Suppression of basal autophagy in neural cells causes neurodegenerative disease in mice. Nature 441:885–889. CrossRef Medline

Hindle S, Hebbar S, Sweeney ST (2011) Invertebrate models of lysosomal storage disease: what have we learned so far? Invert Neurosci 11:59–71. CrossRef Medline

Juhász G, Erdi B, Sass M, Neufeld TP (2007) Atg7-dependent autophagy promotes neuronal health, stress tolerance, and longevity but is dispensable for metamorphosis in *Drosophila*. Genes Dev 21:3061–3066. CrossRef Medline

Kinghorn KJ (2011) Pathological looping in the synucleinopathies: investigating the link between Parkinson's disease and Gaucher disease. Dis Model Mech 4:713–715. CrossRef Medline

Kinghorn KJ, Castillo-Quan JI, Bartolome F, Angelova PR, Li L, Pope S, Cochemé HM, Khan S, Asghari S, Bhatia KP, Hardy J, Abramov AY, Partridge L (2015) Loss of PLA2G6 leads to elevated mitochondrial lipid peroxidation and mitochondrial dysfunction. Brain 138:1801–1816. CrossRef Medline

Komatsu M, Waguri S, Chiba T, Murata S, Iwata J, Tanida I, Ueno T, Koike M, Uchiyama Y, Kominami E, Tanaka K (2006) Loss of autophagy in the central nervous system causes neurodegeneration in mice. Nature 441:880–884. CrossRef Medline

Li M, Khambu B, Zhang H, Kang JH, Chen X, Chen D, Vollmer L, Liu PQ, Vogt A, Yin XM (2013) Suppression of lysosome function induces autophagy via a feedback down-regulation of MTOR complex 1 (MTORC1) activity. J Biol Chem 288:35769–35780. CrossRef Medline

Malagelada C, Jin ZH, Jackson-Lewis V, Przedborski S, Greene LA (2010) Rapamycin protects against neuron death in vitro and in vivo models of Parkinson's disease. J Neurosci 30:1166–1175. CrossRef Medline

Maor G, Rencus-Lazar S, Filocamo M, Steller H, Segal D, Horowitz M (2013) Unfolded protein response in Gaucher disease: from human to *Drosophila*. Orphanet J Rare Dis 8:1–14. CrossRef Medline

Maor G, Cabasso O, Krivoruk O, Rodriguez J, Steller H, Segal D, Horowitz M (2016) The contribution of mutant *GBA* to the development of Parkinson disease in *Drosophila.* Hum Mol Genet. Advance online publication. Retrieved May 9, 2016. doi: 10.1093/hmg/ddw129. CrossRef Medline

Mills K, Eaton S, Ledger V, Young E, Winchester B (2005) The synthesis of internal standards for the quantitative determination of sphingolipids by tandem mass spectrometry. Rapid Commun Mass Spectrom 19:1739–1748. CrossRef Medline

Myllykangas L, Tyynelä J, Page-McCaw A, Rubin GM, Haltia MJ, Feany MB (2005) Cathepsin D-deficient *Drosophila* recapitulate the key features of neuronal ceroid lipofuscinoses. Neurobiol Dis 19:194–199. CrossRef Medline

Orvisky E, Park JK, LaMarca ME, Ginns EI, Martin BM, Tayebi N, Sidransky E (2002) Glucosylsphingosine accumulation in tissues from patients with Gaucher disease: correlation with phenotype and genotype. Mol Genet Metab 76:262–270. CrossRef Medline

Osellame LD, Rahim AA, Hargreaves IP, Gegg ME, Richard-Londt A, Brandner S, Waddington SN, Schapira AH, Duchen MR (2013) Mitochondria and quality control defects in a mouse model of Gaucher disease: links to Parkinson's disease. Cell Metab 17:941–953. CrossRef Medline

Palikaras K, Tavernarakis N (2012) Mitophagy in neurodegeneration and aging. Front Genet 3:297. CrossRef Medline

Ravikumar B, Sarkar S, Davies JE, Futter M, Garcia-Arencibia M, Green-Thompson ZW, Jimenez-Sanchez M, Korolchuk VI, Lichtenberg M, Luo S, Massey DC, Menzies FM, Moreau K, Narayanan U, Renna M, Siddiqi FH, Underwood BR, Winslow AR, Rubinsztein DC (2010) Regulation of mammalian autophagy in physiology and pathophysiology. Physiol Rev:1383–1435.

Rera M, Bahadorani S, Cho J, Koehler CL, Ulgherait M, Hur JH, Ansari WS, Lo T Jr, Jones DL, Walker DW (2011) Modulation of longevity and tissue homeostasis by the *Drosophila* PGC-1 homolog. Cell Metab 14:623–634. CrossRef Medline

Robinson SW, Herzyk P, Dow JA, Leader DP (2013) FlyAtlas: database of gene expression in the tissues of *Drosophila melanogaster*. Nucleic Acids Res 41:D744–D750. CrossRef Medline

Roczniak-Ferguson A, Petit CS, Froehlich F, Qian S, Ky J, Angarola B, Walther TC, Ferguson SM (2012) The transcription factor TFEB links mTORC1 signaling to transcriptional control of lysosome homeostasis. Sci Signal 5:ra42. CrossRef Medline

Rogov V, Dötsch V, Johansen T, Kirkin V (2014) Interactions between autophagy receptors and ubiquitin-like proteins form the molecular basis for selective autophagy. Mol Cell 53:167–178. CrossRef Medline

Rubinsztein DC, Shpilka T, Elazar Z (2012) Mechanisms of autophagosome biogenesis. Curr Biol 22:R29–R34. CrossRef Medline

Shults CW (2006) Lewy bodies. Proc Natl Acad Sci U S A 103:1661–1668. CrossRef Medline

Sidransky E (2004) Gaucher disease: complexity in a "simple" disorder. Mol Genet Metab 83:6–15. CrossRef Medline

Sofola-Adesakin O, Castillo-Quan JI, Rallis C, Tain LS, Bjedov I, Rogers I, Li L, Martinez P, Khericha M, Cabecinha M, Bahler J, Partridge L (2014) Lithium suppresses Ab pathology by inhibiting translation in an adult *Drosophila* model of Alzheimer's disease. Front Aging Neurosci 6:1–10. CrossRef Medline

Suzuki M, Fujikake N, Takeuchi T, Kohyama-Koganeya A, Nakajima K, Hirabayashi Y, Wada K, Nagai Y (2015) Glucocerebrosidase deficiency accelerates the accumulation of proteinase K-resistant α-synuclein and aggravates neurodegeneration in a *Drosophila* model of Parkinson's disease. Hum Mol Genet 24:6675–6686. CrossRef Medline

Tatar M, Post S, Yu K (2014) Nutrient control of *Drosophila* longevity. Trends Endocrinol Metab 25:509–517. CrossRef Medline

Tognon E, Kobia F, Busi I, Fumagalli A, De Masi F, Vaccari T (2016) Control of lysosomal biogenesis and Notch-dependent tissue patterning by components of the TFEB-V-ATPase axis in *Drosophila melanogaster*. Autophagy 12:499–514. CrossRef Medline

Wagh DA, Rasse TM, Asan E, Hofbauer A, Schwenkert I, Dürrbeck H, Buchner S, Dabauvalle MC, Schmidt M, Qin G, Wichmann C, Kittel R, Sigrist SJ, Buchner E (2006) Bruchpilot, a protein with homology to ELKS/CAST, is required for structural integrity and function of synaptic active zones in *Drosophila*. Neuron 49:833–844. CrossRef Medline

Wong R, Piper MD, Wertheim B, Partridge L (2009) Quantification of food intake in *Drosophila*. PLoS One 4:e6063. CrossRef Medline

Xu H, Ren D (2015) Lysosomal physiology. Annu Rev Physiol 77:57–80. CrossRef Medline

Xu YH, Xu K, Sun Y, Liou B, Quinn B, Li RH, Xue L, Zhang W, Setchell KD, Witte D, Grabowski GA (2014) Multiple pathogenic proteins implicated in neuronopathic Gaucher disease mice. Hum Mol Genet 23:3943–3957. CrossRef Medline

Yu L, McPhee CK, Zheng L, Mardones GA, Rong Y, Peng J, Mi N, Zhao Y, Liu Z, Wan F, Hailey DW, Oorschot V, Klumperman J, Baehrecke EH, Lenardo MJ (2010) Termination of autophagy and reformation of lysosomes regulated by mTOR. Nature 465:942–946. CrossRef Medline

Zatloukal K, Stumptner C, Fuchsbichler A, Heid H, Schnoelzer M, Kenner L, Kleinert R, Prinz M, Aguzzi A, Denk H (2002) p62 is a common component of cytoplasmic inclusions in protein aggregation diseases. Am J Pathol 160:255–263. CrossRef Medline

Zoncu R, Bar-Peled L, Efeyan A, Wang S, Sancak Y, Sabatini DM (2011) mTORC1 senses lysosomal amino acids through an inside-out mechanism that requires the vacuolar H(+)-ATPase. Science 334:678–683. CrossRef Medline